J. Fluid Mech. (2004), *vol.* 521, *pp.* 35–68.
DOI: 10.1017/S0022112004000813 Printed in the United Kingdom

Parametric study of noise from dual-stream nozzles

By K. VISWANATHAN

The Boeing Company, MS 67-ML, PO Box 3707, Seattle, WA 98124-2207, USA
k.viswanathan@boeing.com

(Received 21 November 2002 and in revised form 2 June 2004)

A detailed parametric study of the noise from dual-stream jets has been carried out to assess the importance of the noise generated by the primary and secondary shear layers and their principal radiation directions under different operating conditions. Realistic geometries and engine conditions are chosen to enhance the relevance and the usefulness of the experimental results reported here. The effects of different operating conditions in the two streams on both the turbulent mixing noise and shock-associated noise are evaluated under static conditions as well as in the presence of an external co-flowing stream. The results indicate that the secondary-to-primary jet velocity ratio is an important parameter for mixing noise while its effect is negligible on shock-associated noise. The shock-associated noise, not surprisingly, is dependent on the geometric details of the nozzle. The characteristics of this noise component are very different depending on whether shocks are present in the primary or secondary stream. There is strong radiation of shock noise to the aft angles when the secondary stream is supersonic. This trend is troublesome since this component is transmitted into the aft cabin of certain aircraft with engines mounted close to the fuselage. The intensity of the shock-associated noise at the lower angles, in general, is proportional to the strength of the shocks and scales with $(M_p^2 - M_d^2)^2$ or $(M_s^2 - M_d^2)^2$ (M_p and M_s denote the Mach numbers of the primary and secondary streams and M_d is the design Mach number). Just as for a single jet, the effect of forward flight on mixing noise and shock-associated noise is very different. While there is a progressive reduction in levels of mixing noise with increasing free-stream velocity, there is amplification of the shock-associated noise. This is particularly so for the aft-radiated component of shock noise from the secondary stream. This effect could further exacerbate the interior noise in the aft cabin.

1. Introduction

Aircraft noise is an unwanted and annoying byproduct of aviation. The growth in operations of aircraft throughout the world has led to an ever-increasing level of this nuisance and more and more people are impacted by aircraft noise. The introduction of the jet engine as the preferred propulsion system highlighted the problem of jet noise. The extremely high noise levels of the small military jet engines needed to be significantly reduced before larger jet-powered aircraft could be introduced into civilian service. This need motivated initial attempts at noise reduction in the late 1940s and early 1950s. Since that time, considerable research activity has been undertaken to understand the generation and propagation of jet noise, as well as to devise techniques for its reduction. The initial work, based on close observation of

experimental data and formulation of a suitable theory, was directed at gaining a fundamental understanding of the noise generation mechanisms.

The need for reduction of jet noise for subsonic commercial jets, and hence the emphasis on jet noise research, has varied with the evolution of engine technology. Turbojet engines, with very high jet noise levels, powered the earliest jet aircraft. The introduction of fuel-efficient low-bypass-ratio turbofan engines in the early 1960s reduced the jet noise, but made fan noise an equally important component of the total aircraft noise. Better nacelle designs incorporating acoustic lining reduced the fan noise. Consequently, the jet noise from these engines became the dominant noise component once again. The launch of the wide-body jet transport in the late 1960s necessitated the development of a more powerful, yet quieter, engine. This requirement led to the introduction of the high-bypass-ratio turbofan engines and there was a dramatic decrease in both jet and fan noise. With a bypass ratio greater than 5.0, the jet exhaust velocity was reduced to subsonic levels even at takeoff power. Due to the lower jet velocity, the importance of jet noise became secondary and fan noise became the major contributor to overall noise. There has been only minimal reduction of jet noise since that time and most of the research efforts have concentrated on the reduction of noise from fans of ever-increasing diameter. Major advances in lining technology and the incorporation of designs for low noise have yielded steady reduction of fan noise in the last two decades. Though further increases in bypass ratio would yield a lower jet noise, manufacturing problems associated with larger fans and the compatibility of larger diameter engines with existing aircraft configurations might preclude the widespread use of these types of engines, see Reed, Bhat & Conley (1999).

The thrust requirement from jet engines has been increasing steadily, as larger airplanes and derivative airplanes with increased gross weight have been introduced into service. However, the bypass ratio of most engines in commercial service has not changed significantly. The increased thrust has mainly been achieved by operating the engines at higher nozzle pressure ratios (NPR), with the attendant higher jet velocities. One can appreciate this trend by comparing the current engine cycles at takeoff with those of the early 1970s. The recent adoption of more stringent rules for community noise has brought the problem of high levels of jet noise back to the forefront, as it is realized that a reduction of overall aircraft noise would require a significant reduction of jet noise. This has led to renewed interest in the noise of dual-stream jets and the development of designs for noise reduction.

The exhaust of a turbofan engine is characterized by a host of parameters: primary nozzle pressure ratio, primary temperature, secondary nozzle pressure ratio, secondary temperature, secondary-to-primary jet velocity ratio (V_s/V_p), and secondary-to-primary nozzle area ratio (A_s/A_p). The subscripts p and s denote primary (core) and secondary (fan) streams, respectively. The noise from a dual-stream nozzle is dependent on the above thermodynamic and geometric parameters, which define the noise sources. Conceptually, one could visualize three distinct noise sources: the inner shear layer between the primary and secondary streams, the outer shear layer between the secondary and ambient streams, and the fully merged jet farther downstream, with characteristic length and velocity scales being different for each source.

Detailed experimental studies, to understand the characteristics of the different sources, were carried out in the 1970s at Lockheed, GE Aircraft Engines, Pratt and Whitney (as reported in several NASA Contractor Reports and Air Force Aero Propulsion Laboratory Reports), NASA, Boeing, Rolls Royce and the National Gas Turbine Establishment. The following brief list of references documents some

of these experimental studies: Williams, Ali & Anderson (1969), Dosanjh, Yu & Abdelhamid (1971), Dosanjh, Bhutiani & Ahuja (1978), Olsen & Friedman (1974), Cocking (1976), Kozlowski & Packman (1976), Crouch, Coughlin & Paynter (1976), Knott *et al.* (1978), Goodykoontz & Stone (1979), Tanna, Tester & Lau (1979), Tanna (1980), Lu (1983), Tanna & Morris (1985), Salikuddin (1995), Fisher, Preston & Mead (1998*a*, *b*) and the reports from the NASA Advanced Subsonic Technology (AST) program.

There have also been numerous attempts at the development of a prediction method for jet noise from dual-stream nozzles that would be applicable over a wide range of jet operating conditions. These have ranged in complexity, with simple expressions for the total radiated power to very complicated empirical formulations for the noise spectra. Although jet engines have dominated civil aviation for several decades, there is still no prediction method based on first principles. The basic lack of quantitative understanding has precluded the development of a prediction theory even for a single-stream jet. For dual-stream jets, the large number of aerodynamic and geometric parameters compounds this problem. Installation effects, asymmetry caused by struts and pylons needed for engine mounting and wing upwash produce complicated effects, which further confound noise prediction from an engine installed on an aircraft. Detailed spectral information over a wide range of angles is required for practical applications and it is in this regard that most methodologies for prediction fall short. Most methods for noise prediction used by the industry are based on empirical correlations of measured data. This is not to imply that these are just curve fits; rather, models are developed based on much of the accepted theory, with empirical coefficients providing a good fit with data. It is worth noting that there is no general agreement on a theory for jet noise and hence many of the semi-empirical models are based on a host of assumptions, some of which may not be fully validated. Some of the prediction methods may be found in the following references: Balsa & Gliebe (1977), Stone (1977), Pao (1979), Larson (1979), Stone, Groesbeck & Zola (1983), Tanna & Morris (1985), Lu (1986), the SAE (1994) method which incorporates the formulation of Lu (1986), Fisher *et al.* (1998*a*, *b*), and Stone, Zola & Clark (1999).

In the preliminary-design phase of an aircraft, a conceptual engine that would provide adequate thrust over the flight envelope is selected and the noise characteristics assessed using existing methods. As most of the predictions methods are empirical and rely on experimental databases, it is clear that the quality of the database is critical to the validity of the predictions. A recent analysis of available data on jet noise from different facilities/rigs revealed that many measurements are contaminated by extraneous noise, as reported in Viswanathan (2003, 2004). As discussed in those papers, the issue of data quality is even more paramount in the development of concepts for noise reduction.

Many of the studies performed in the 1970s and the early 1980s concentrated on jets with inverted velocity profiles (IVP, secondary stream faster than the primary stream), as the noise reduction potential of these jets was recognized. Also, these studies were performed in support of the Supersonic Transport (SST) and the Supersonic Cruise Aircraft Research (SCAR) programs, wherein the IVP concept was a viable candidate. However, the complexities and weight penalties associated with ducting the higher velocity stream to the secondary side have proven to be prohibitive and hence the IVP concept has not found application in jet engines. Therefore, a systematic study, with an emphasis on normal velocity profile (NVP) jets, is described here that sheds light on the mechanisms of generation of noise from dual-stream nozzles.

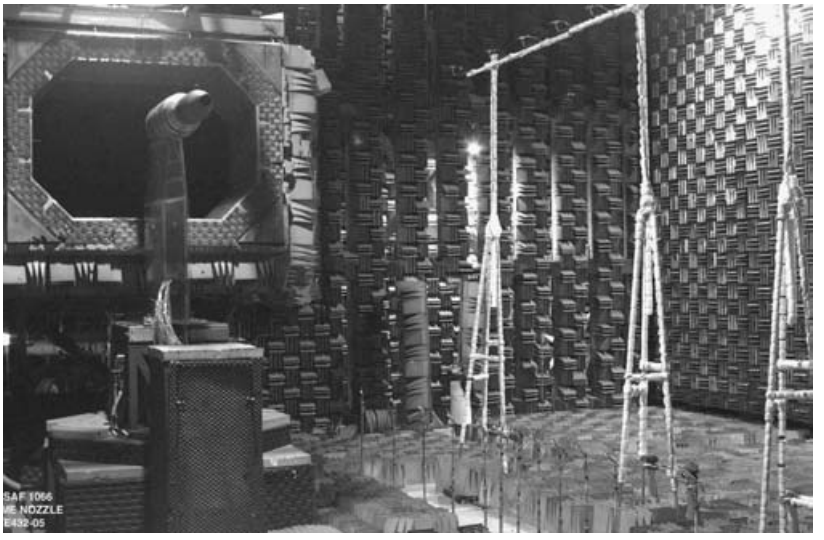

FIGURE 1. Photograph of LSAF showing the anechoic chamber, jet rig, wind tunnel and some of the microphones.

2. Experimental program

The experiments have been performed in the Low Speed Aeroacoustic Facility (LSAF) at Boeing, with simultaneous measurement of thrust and noise. Detailed descriptions of the test facility, the jet simulator, the data acquisition and reduction process, etc. may be found in Viswanathan (2003). Figure 1 shows a picture of the anechoic chamber, the jet simulator, the wind tunnel and some of the microphones. The jet simulator is embedded in an open-jet wind tunnel, which can provide a maximum free-stream Mach number of 0.32. The microphones are laid out at a constant sideline distance of 15 ft (4.572 m) from the jet axis, except the microphone at 155°, which is at a distance of 12.75 ft (3.886 m). All angles are measured from the jet inlet axis, with a polar angular range of 50° to 155°. Additional microphones are also located at several polar angles at different azimuthal angles. Narrowband data with a bandwidth of 23.4 Hz are acquired and synthesized to produce 1/3-octave spectra, up to a centre band frequency of 80 000 Hz. All the data have been corrected to a common distance of 20 ft (6.096 m) from the centre of the nozzle exit (coordinate system with origin at the centre of the nozzle exit) and standard-day conditions: an ambient temperature of 77 °F (298 K) and a relative humidity of 70%. The atmospheric attenuation is calculated using the method of Shields & Bass (1977).

The area ratio of the nozzle selected for this study is 3.0, which is representative of the area ratio of the larger jet engines in service. The area of the primary nozzle is 4.714 in.^{2} (0.00304 m^2) and that of the secondary nozzle is 14.143 in.^{2} (0.00912 m^2). The primary nozzle extends beyond the secondary nozzle and the geometry is again typical of existing configurations. Since the main goal of this study is to enhance our understanding of the physical mechanisms, clean internal lines without struts, bifurcations, etc., are maintained so as to avoid complexities associated with asymmetries and other effects. Once the geometry is fixed, there are four thermodynamic variables, namely the total pressures and temperatures in the two streams that may be varied independently. However, in order to keep the text matrix reasonably small, the temperature of the secondary stream is always maintained at

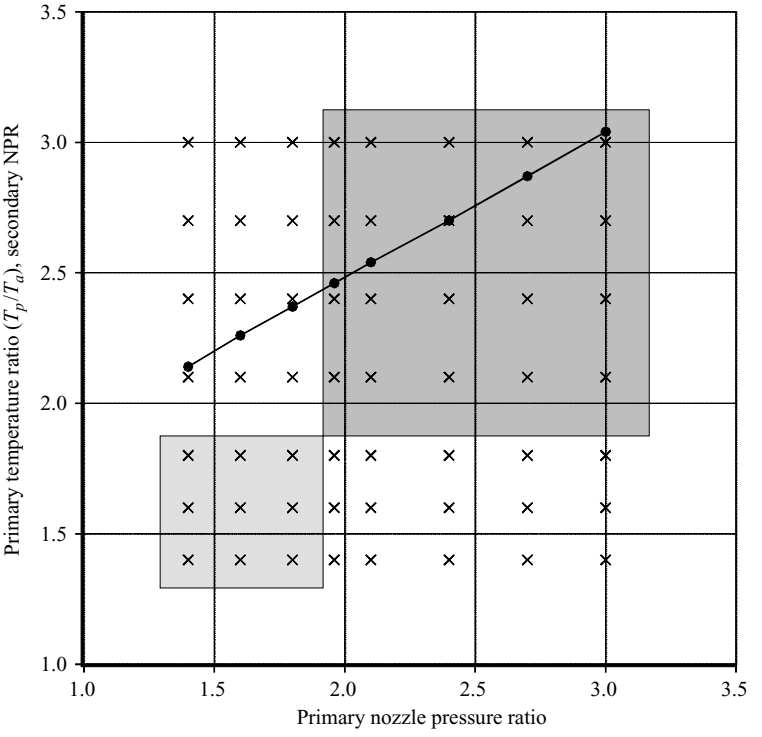

FIGURE 2. Test matrix of the experimental program. Lighter grey: both streams subsonic; darker grey: both streams supersonic. •, T_p/T_a; ×, NPR_s.

ambient temperature. The value of the secondary temperature ratio (T_s/T_a, where T denotes total temperature) for most engines is ∼1.15. Hence, the above choice is not too restrictive. When tests are carried out for actual engine geometries, the thermodynamic variables are set so as to match a given engine cycle. In order to ensure practical relevance, a typical engine cycle that has a fixed total temperature for a specified NPR is chosen for the primary stream. The NPR of the primary stream spans a range of 1.4 to 3.0, with a corresponding temperature ratio range (T_p/T_a) of 2.14 to 3.04. At every cycle point for the primary flow, the NPR in the secondary stream is systematically varied over a range of 1.4 to 3.0. In addition, data are acquired with the primary jet unheated at the above cycle points. The basic test matrix is shown in figure 2. The dark circles and the line define the test points of the primary jet, namely NPR_p and (T_p/T_a). The crosses denote the NPR in the secondary stream, NPR_s. Thus, an extensive database has been generated to provide high-quality data for the evaluation and improvement of prediction methods for jet noise.

The issue of comparing noise data on an equivalent basis wherein the levels are normalized for constant thrust, mass flow and flow area, addressed by Tanna (1980) for example, is not considered even though thrust measurements have been made. The rationale for the choice of the current test matrix and the presentation of scale-model noise data at the test points shown in figure 2 is as follows. First, in a real turbofan engine the total temperature of the primary stream increases with increasing pressure ratio. Typically, the engine power setting is represented by the corrected rotational speed of the fan. The fan operating line is particular to a given engine and is based on the details of the design of the turbo machinery, such as the number of compressor and

turbine stages, number of spools, etc. These features are guided by the design practices and philosophies of the engine companies. As the fan speed is increased, the primary pressure ratio, the primary total temperature, the fan pressure ratio and the thrust increase. However, in order to maintain constant thrust, mass flow and flow area as was done in Tanna (1980) and Tanna & Morris (1985), the thermodynamic variables in the two streams must be adjusted in a way that does not represent the operational characteristics of real engines. For example, the examination of the effect of varying the velocity ratio (V_s/V_p) on noise while holding the static temperature ratio constant would entail the selection of the following trends for the thermodynamic variables: for increasing NPR of the primary stream, the temperature of the primary stream and the NPR of the secondary stream would have to decrease. The current test matrix aims to simulate realistic engine operation and is not structured to produce constant static temperature and velocity ratios as was done in Tanna & Morris (1985), as the intent of that study was to isolate the effects of source alteration from that of the flow/acoustic interaction. Thus, this experimental program complements the previous studies. One could attempt to scale the noise data for constant thrust, for example. However, the noise level is a strong function of bypass ratio and the same total thrust could be obtained by numerous combinations of the pressure ratios in the two streams. Further, in a real turbofan engine, the bypass ratio continues to increase as the fan speed is decreased. Therefore, it is not as straightforward to scale data as for a single jet while replicating the thermodynamic cycle of a turbofan engine.

It is worth noting that some of the past experimental studies also attempted to achieve the objective of quantifying the effects of varying the cycle conditions. However, the parametric variation was not very extensive and the quality of the acoustic data was suspect. The experimental program of Salikuddin (1995) was similar in scope to the current one, though the emphasis of that test was on shock-associated noise. The primary objective of the test program is the assessment of the importance of the noise generated by the inner and outer shear layers and their principal radiation directions under different operating conditions. To this end, data have been acquired at both sub-critical and super-critical pressure ratios. The main results from the current experimental program are presented in the following sections.

Detailed flow field measurements would be very valuable and complement the aeroacoustic results. Insights provided by the changes in flow, and how they relate to the observed trends in the radiated noise, could potentially enhance the development of noise reduction concepts. However, such measurements are quite complicated and beyond the scope of this study. In order to relate the features of the flow to noise, comprehensive data on the mean flow quantities such as velocities and temperatures, turbulence quantities such as the turbulent fluctuations, two-point space-time correlations, etc. must be acquired over a substantial volume of the jet plume. Only recently have such measurements become feasible, albeit with limitations, due to advances in instrumentation and optical techniques; see for example Bridges (2002), Bridges & Wernet (2003), and Seiner (2003). Given the prohibitive cost of acquiring and maintaining the expertise and the equipment, such measurements are not undertaken by the aerospace industry anymore and are confined to NASA and research laboratories in a few universities. These emerging flow field data would eventually lead to better physical models of the noise generation mechanisms.

The high quality of acoustic data obtained with the current jet rig after several improvements was established through good agreement with data obtained with a blow-down tunnel using the same nozzles, as reported in Viswanathan (2003). Sample comparisons were shown over a range of power settings. Additional comparisons at

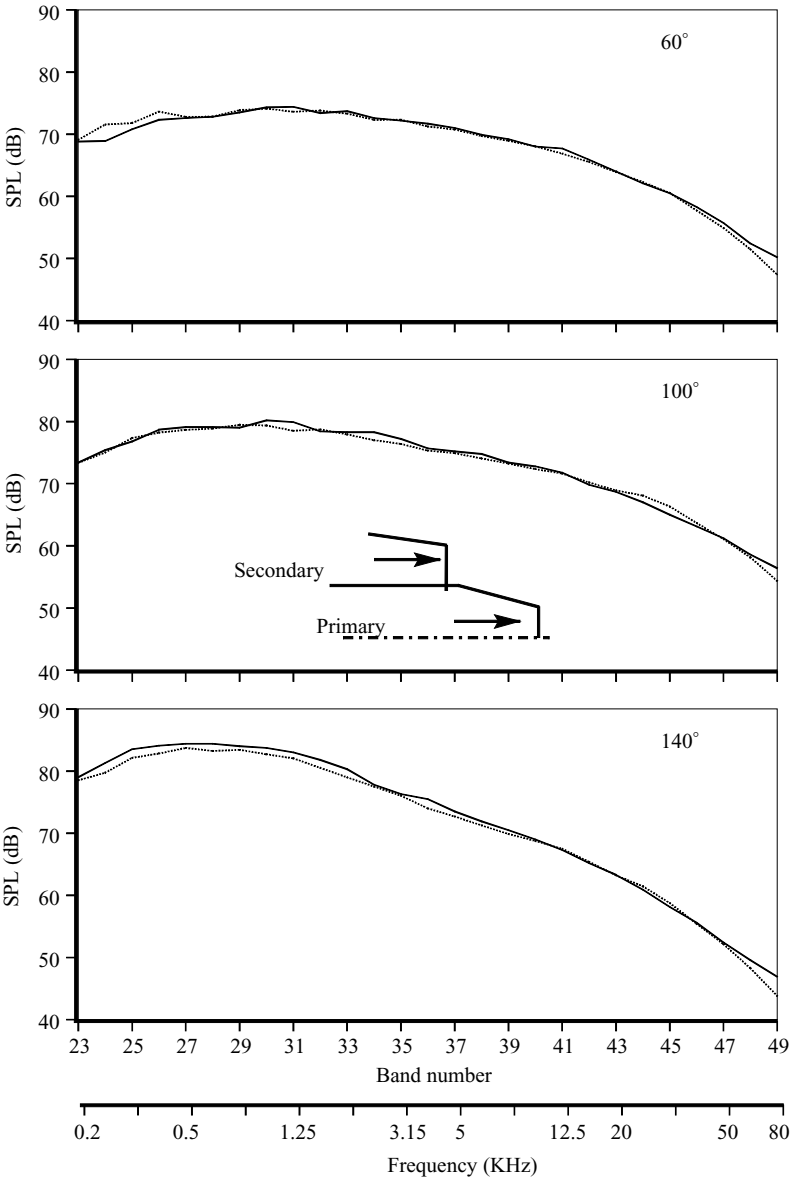

FIGURE 3. Comparison of spectra at various polar angles (measured with respect to the inlet axis). $NPR_p = 1.16$, $T_p = 1152\,^{\circ}\mathrm{R}$ (640 K), $NPR_s = 1.26$, $T_s = 540\,^{\circ}\mathrm{R}$ (300 K). Solid line, quiet dual flow rig (blow-down facility); dashed line, current jet rig.

lower power settings have also been carried out to eliminate any doubts about the validity of the results presented here. A sample test case is shown in figure 3. The cycle conditions are: $NPR_p = 1.16$, $T_p = 1152\,^{\circ}\mathrm{R}$ (640 K), $NPR_s = 1.26$, $T_s = 540\,^{\circ}\mathrm{R}$ (300 K). The current measurements are in excellent spectral agreement with data obtained with the Quiet Dual Flow Rig (QDFR) at all the angles. Attention is drawn to some tones at frequencies below 400 Hz (band number 26), which are more perceptible at lower angles. These tones are more pronounced in the following figures. They are facility-related as discussed in Viswanathan (2003) and should be removed, as they

are not part of jet noise. However, here, as-measured data are presented without the subtraction of these tones.

The test matrix (in figure 2) has been chosen to ascertain the effects of parametric variations on both the turbulent mixing noise and shock-associated noise. At takeoff, the engines on an aircraft are operated at close to maximum power; once airborne and after the plane has reached a safe altitude, the engines are throttled back to reduce noise at the cutback microphone and for the communities living down-range. Then the plane is accelerated to cruise altitude with maximum power. At cruise, the nozzles are operated at supersonic pressure ratios because of the lower ambient pressure. And at approach, the engines are operated at low powers. Thus, an engine operates over a wide range of power settings in a typical flight. The results presented in this paper, over a wide range of nozzle pressure ratios and jet velocities, thus encompass all facets of the flight envelope. However, in the interest of keeping the paper to a reasonable length, the experimental results are split into three parts. Salient results for the turbulent mixing noise are presented in an Appendix,† while new findings on shock-associated noise are presented in § 4. In § 5 the effects of forward flight on both mixing and shock-associated noise are presented. It is further noted that though the results for the turbulent mixing noise are not entirely new, three important reasons justify their inclusion: (i) extension of the range of the Strouhal number through the use of a relatively large nozzle and the acquisition of good data up to 80 kHz in the test, (ii) the possibility for the refinement of theoretical and semi-empirical prediction methods afforded by the controlled parametric variation, and (iii) the careful quantification of the effect of forward flight, which is essential for the projection of engine static data to equivalent flyover conditions in order to obtain good agreement with flight test data. This is an extremely important issue for aircraft noise certification.

3. Shock-associated noise

It is well-established that shock-associated noise is important for supersonic jets that are expanded imperfectly. The intensity of shock noise is dependent on the degree of mismatch between the design Mach number (M_d) and the fully expanded jet Mach number (M_j). The relative importance of the broadband shock-associated noise and turbulent mixing noise is a strong function of radiation angle and jet operating conditions. For a fixed Mach number, the turbulent mixing noise level increases as the jet temperature is increased, while the amplitude of the broadband shock-associated noise remains nearly unaltered. Hence, the magnitude of the shock noise increase over the mixing noise is a maximum for cold jets. The shock noise radiation is omni-directional, while the mixing noise is radiated principally to the aft directions. The jet temperature then sets the relative levels of the two components. In general, shock-associated noise is more pronounced in the forward quadrant, and is distinguished easily since the levels of turbulent mixing noise are low in these directions. Since the pioneering work of Harper-Bourne & Fisher (1973), there have been several investigations of shock-associated noise, for example Seiner & Norum (1979, 1980), Norum & Seiner (1982*a*, *b*), Tam & Tanna (1982), Seiner (1984), and Yamamoto *et al.* (1984). In the theoretical arena, seminal research by Tam & Tanna (1982) and Tam (1987) has helped to clarify the physical mechanisms responsible for

† Available as a supplement to the online version, or from the author or the JFM Editorial office, Cambridge.

the generation of shock-associated noise. According to their theory, this component of noise is generated by the weak but coherent interaction between the large-scale turbulent structures in the jet shear layer and the quasi-periodic shock cell system. Formulae for the peak frequency and intensity were also developed. A prediction method based on this theory was able to reproduce the observed characteristics very well. For a comprehensive treatment of this topic see Tam (1991) and the references therein. However, all the above studies were restricted to single-stream nozzles.

Most commercial jet engines have fixed nozzle geometry, with the jet Mach number being subsonic during takeoff. During climb and at cruise, the ambient pressure is much lower than at sea level and the nozzle is invariably operated at supersonic conditions, generating shock noise. Broadband shock-associated noise is a concern during this portion of the flight envelope for certain aircraft, as this component impinges on the fuselage and is transmitted into the interior of the aircraft. This is especially so for twin-engine aircraft with engines mounted closer to the fuselage. Current solutions for the reduction of the interior noise levels at the affected seats consist of adding acoustic treatment to the sidewall panel. Efforts at the reduction of the shock noise at the source have not been successful, due to our limited understanding of the shock noise generation mechanism in dual-stream jets. Even though the model of Tam (1987) has been very successful in describing the mechanism of noise generation from single-stream jets, the role of the inner shear layer in a dual-stream jet is not understood. As shown below, the noise characteristics are very different for a dual-stream jet. One of the very few test programs that addressed this problem is that due to Tanna, Brown & Tam (1985). In two companion papers, Tam & Tanna (1985*a*, *b*) provided a theoretical explanation of the observed characteristics from the test program and developed a shock-cell model for the peak frequency and the intensity of the shock-associated noise. Some key differences between the current results and those of Tam & Tanna's study, and possible reasons are examined now.

The effect of operating the primary stream supersonically is first presented. Spectral information (in power spectra or 1/3-octave spectra for turbulent mixing noise) over a wide range of angles is presented to illustrate the effects of the parametric variation. In figure 4, the secondary stream is operated at a nozzle pressure ratio of 2.1, while the primary stream is varied as follows: $NPR_p = 1.8$ and $T_p/T_a = 2.37$, $NPR_p = 2.1$, $T_p/T_a = 2.54$, $NPR_p = 2.4$, $T_p/T_a = 2.70$, and $NPR_p = 2.7$ and $T_p/T_a = 2.87$. As shown in figure 4, there is a gradual change in the spectral shape, noticeable especially at the lower angles, with the shock-associated noise from the primary stream becoming the dominant component. The peak frequency shifts to higher values as we move aft. There is also a substantial increase in the noise at the higher frequencies in the mid-angle range of 120° to 135°. Clearly, as seen in figures A3 (in the Appendix) and 4, the noise from the primary jet controls the total noise when the primary stream is supersonic. When the secondary jet is operated at subsonic Mach numbers (not shown here) similar trends are observed. The noise from the secondary shear layer is evidently unimportant once strong shocks are established in the primary jet.

In the next set of data, the Mach number of the primary stream is maintained at a low supersonic value ($M_p = 1.04$, $T_p/T_a = 2.46$) and the Mach number of the secondary stream is increased. Figure 5 shows the effect on the spectra when the secondary stream is varied as follows: $NPR_s = 1.8$ ($M_s = 0.96$), $NPR_s = 2.4$ ($M_s = 1.19$) and $NPR_s = 3.0$ ($M_s = 1.36$). There are significant differences when the secondary stream becomes supersonic, compared with either a subsonic secondary stream or a supersonic primary stream. In the forward quadrant, the contribution of the shock noise is obvious, as the shock-associated noise is significantly higher than the mixing noise when the Mach

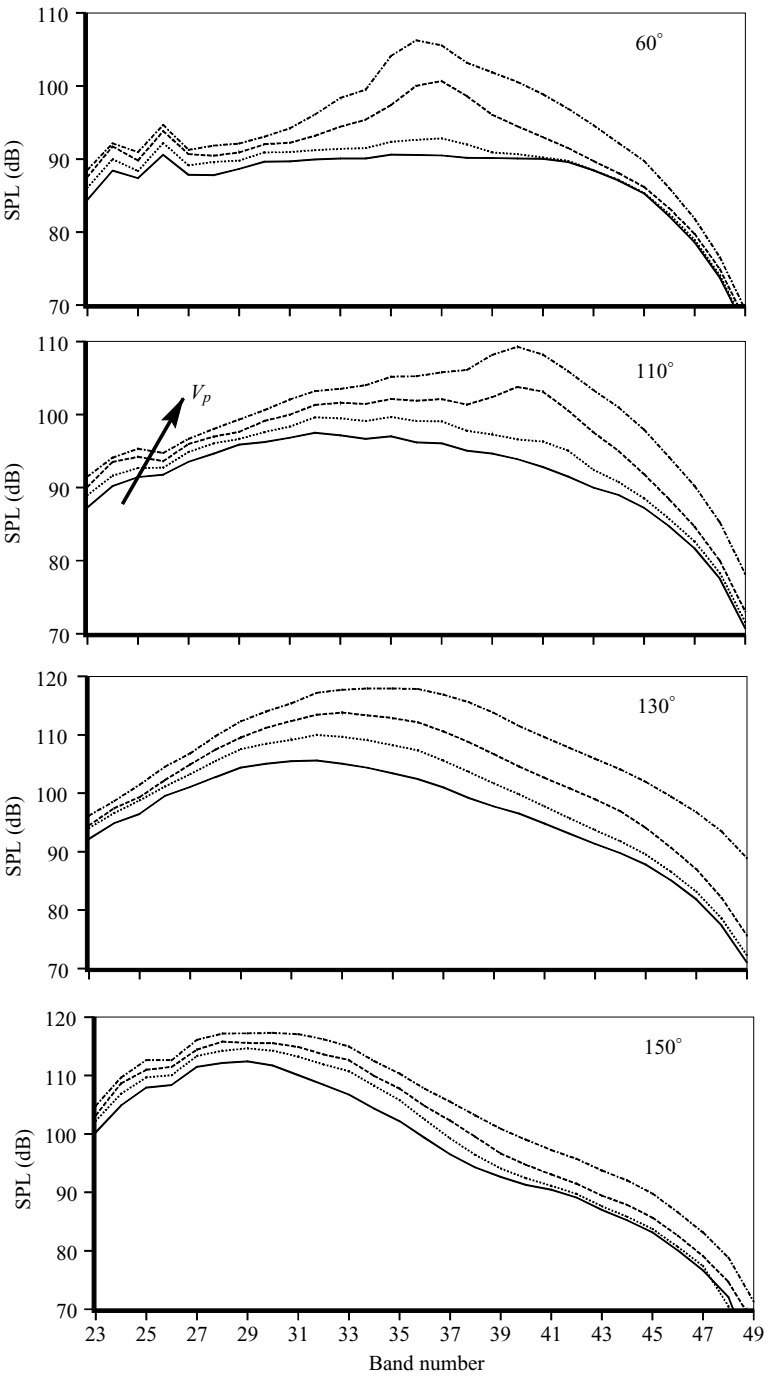

FIGURE 4. Spectral variation due to change in primary stream with fixed secondary jet conditions. $NPR_s = 2.1$, $T_s/T_a = 1.0$. Solid line, $NPR_p = 1.8$, $T_p/T_a = 2.37$ $(V_s/V_p = 0.72)$; dotted line, $NPR_p = 2.1$, $T_p/T_a = 2.54$ $(V_s/V_p = 0.62)$; dashed line, $NPR_p = 2.4$, $T_p/T_a = 2.7$ $(V_s/V_p = 0.56)$; dot-dashed line, $NPR_p = 2.7$, $T_p/T_a = 2.87$ $(V_s/V_p = 0.51)$.

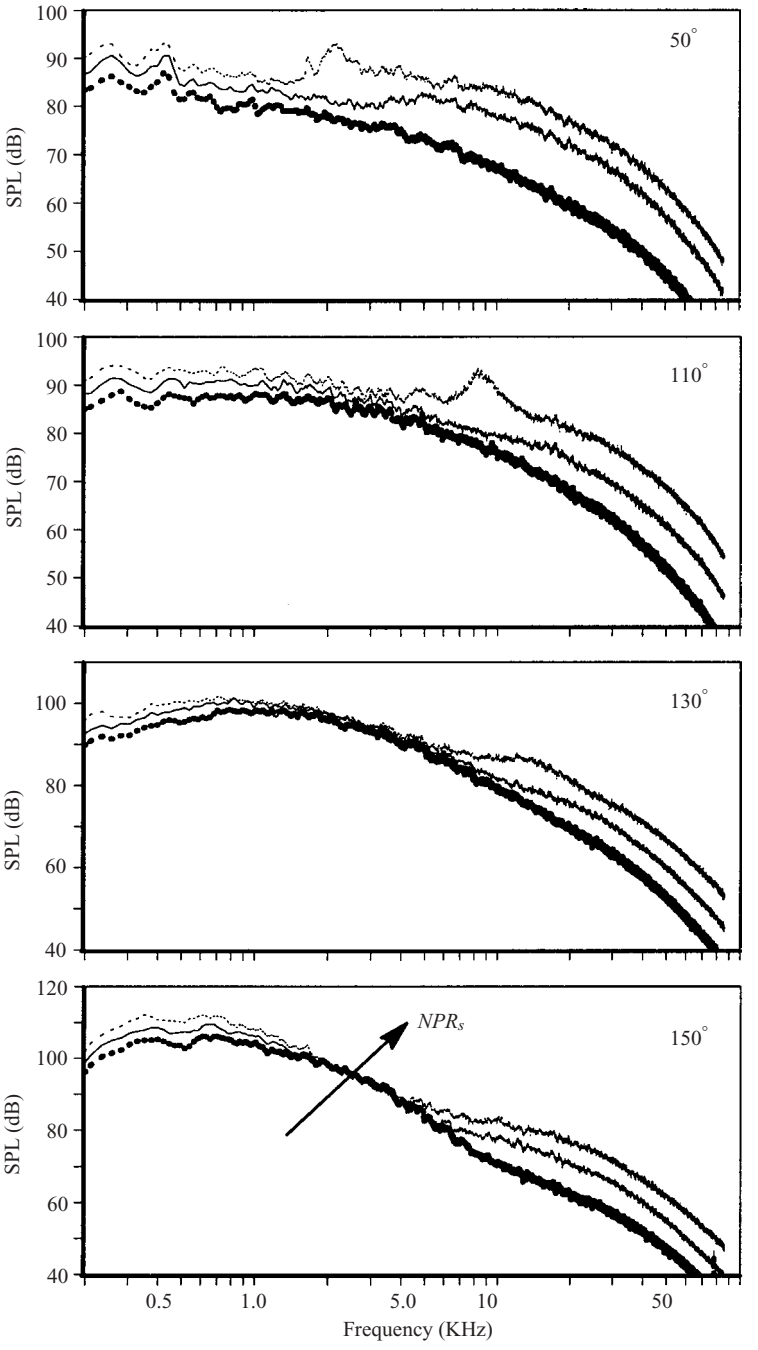

FIGURE 5. Spectral variation due to change in secondary stream with fixed primary jet conditions. $NPR_p = 1.96$, $T_p/T_a = 2.46$, $T_s/T_a = 1.0$. Thick dotted line, $NPR_s = 1.8$; solid line, $NPR_s = 2.4$; thin dashed line, $NPR_s = 3.0$.

number of the secondary stream is increased from 0.96 to 1.36. Of greater importance from the standpoint of cabin noise is the emergence of shock-associated noise at aft angles. In these directions, the peak mixing noise at low frequencies increases with

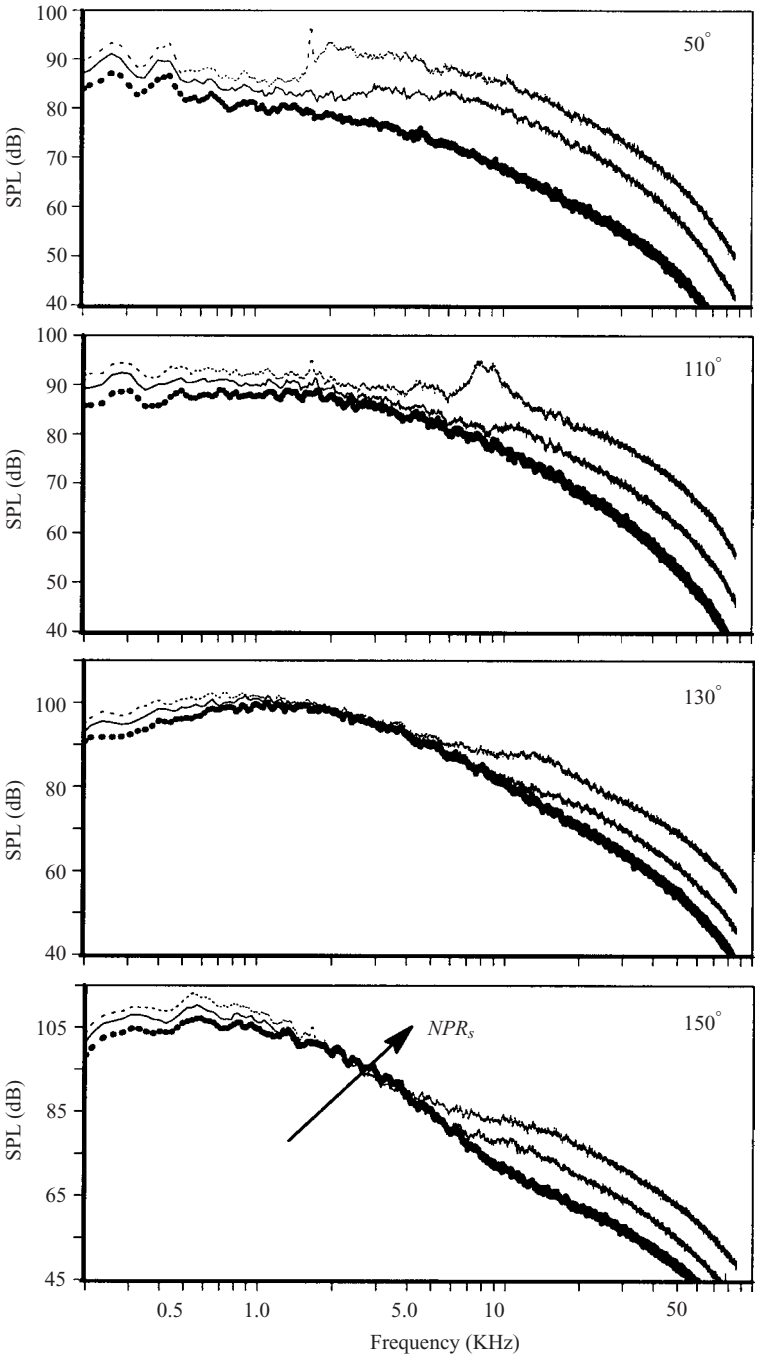

FIGURE 6. Spectral variation due to change in secondary stream with fixed primary jet conditions. $NPR_p = 2.1$, $T_p/T_a = 2.54$, $T_s/T_a = 1.0$. Thick dotted line, $NPR_s = 1.8$; solid line, $NPR_s = 2.4$; thin dashed line, $NPR_s = 3.0$.

increasing mixed jet velocity, as observed earlier. However, there is a second hump at the higher frequencies when the secondary stream becomes supersonic. Similar trends are observed when the Mach number of the primary stream is subsonic, as well as in figure 6 when the Mach number of the primary stream is increased to

1.09 ($NPR_p = 2.1$, $T_p/T_a = 2.54$) and the Mach number of the secondary stream is varied with the same conditions used for figure 5. Note that the Mach number of the primary stream is just supersonic in the above two figures. Comparison of the spectra in figures 4 and 6 brings out the vastly different features of the shock-associated noise, when shocks are present in the primary or secondary streams.

The effect on the spectra of heating the primary jet while holding the primary jet Mach number slightly supersonic for subsonic and supersonic secondary flows are shown in figures 7 and 8, respectively. The temperature ratios T_p/T_a are 1.0, 2.38 and 3.24. In figure 7, with the secondary Mach number subsonic ($M_s = 0.85$), there is a gradual increase in level at the lower angles and a substantial increase of ~15 dB in the peak spectrum level at the aft angles. However, the picture is very different when the secondary Mach number is supersonic ($M_s = 1.28$) in figure 8. The spectral changes at low angles are negligible, ~2 dB across the spectra. Though the low-frequency noise increases in the peak noise direction, again due to the increased mixed jet velocity, there is virtually no change at the higher frequencies. This figure indicates that the shock-associated noise from the secondary stream is dominant, since a large change in the primary velocity associated with heating the jet has negligible effect on radiated noise at high frequencies.

In figure 9, the effect of increasing the secondary Mach number while holding the primary Mach number at a supersonic value ($NPR_p = 3.0$, $M_p = 1.36$) is evaluated. For this primary Mach number there should be strong shocks in the primary jet. As before, the secondary NPR is set as follows: $NPR_s = 1.8$ ($M_s = 0.96$), $NPR_s = 2.1$ ($M_s = 1.09$) and $NPR_s = 3.0$ ($M_s = 1.36$). With the subsonic secondary Mach number, the shock noise seen in the forward angles is due to the primary stream. When the secondary stream becomes supersonic, the shock-associated noise progressively increases at lower angles, by ~8 dB near the peak, and there is a broadening of the spectrum at the peak. There is also an increase in level at all frequencies to the right of the spectral peak. At large angles, the second hump appears when the secondary stream becomes supersonic. The magnitude of the increase in level associated with the shocks in the secondary stream is ~20 dB. It is worth noting that the second hump at the higher frequencies is not present when the primary stream alone is supersonic, as seen in the spectra at the large angles.

Another way of isolating the effects of the different sources is to operate the two streams at a velocity ratio of unity, with and without shocks in the primary stream as follows. In figure 10, spectral comparisons are shown with the secondary stream maintained at a Mach number of 1.09 ($NPR_s = 2.1$), while the primary stream is operated pressure-balanced ($NPR_p = 2.1$) for one case and at $NPR_p = 1.4$ and $T_p/T_a = 2.14$ for the other. At the lower angles, the shock-associated noise due to the primary stream is clearly evident when the primary stream is supersonic. However, there is no change in the spectra at the higher frequencies at all the angles and in the aft directions the noise levels are the same for the two cases. In figure 11, stronger shocks are established as follows: $NPR_s = NPR_p = 3.0$ for one case, while $NPR_s = 3.0$, and $NPR_p = 1.6$ and $T_p/T_a = 2.26$ for the other. Thus the velocity ratio is maintained at unity, with the primary stream subsonic for one case. When the secondary stream alone is supersonic, the contribution of the shock-associated noise from this stream and the appearance of the hump at the higher frequencies in the aft angles are obvious. When both the streams are operated pressure-balanced, the shock peak shifts to lower frequencies. Some alteration of the shock-cell structure in the secondary stream is possibly causing the reduction in the shock peak associated with the secondary stream at 110°. At large aft angles, where the fully mixed jet controls the spectral peak, the levels for the two conditions are similar as expected.

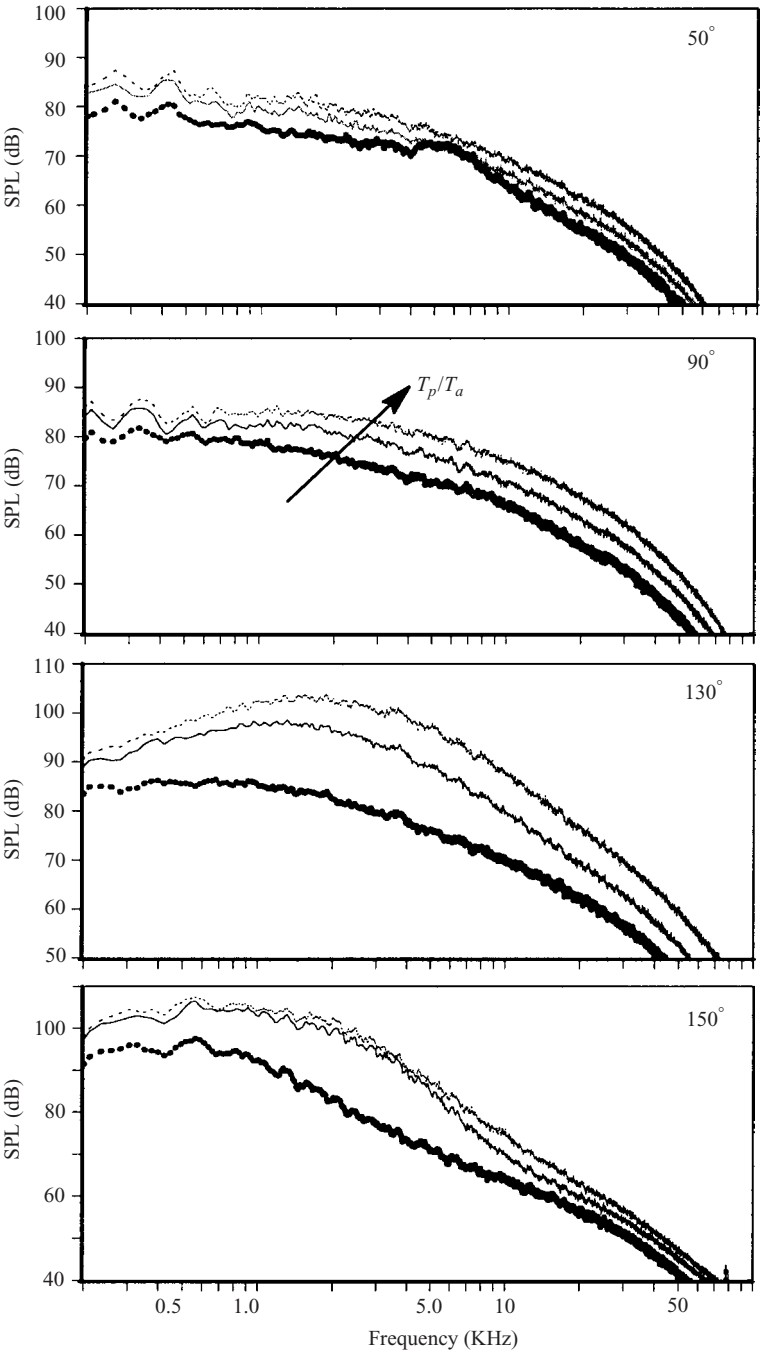

FIGURE 7. Effect of primary jet temperature with fixed secondary jet conditions. $NPR_s = 1.6$, $T_s/T_a = 1.0$, $NPR_p = 2.1$. Thick dotted line, $T_p/T_a = 1.0$ ($V_s/V_p = 0.81$); solid line, $T_p/T_a = 2.38$ ($V_s/V_p = 0.52$); thin dashed line, $T_p/T_a = 3.24$ ($V_s/V_p = 0.45$).

Figures 5–9 highlight the importance of the shock-associated noise from the secondary stream. The experimental program of Tanna *et al.* (1985) indicated that the noise radiated by a dual-stream jet attained a minimum when the Mach number

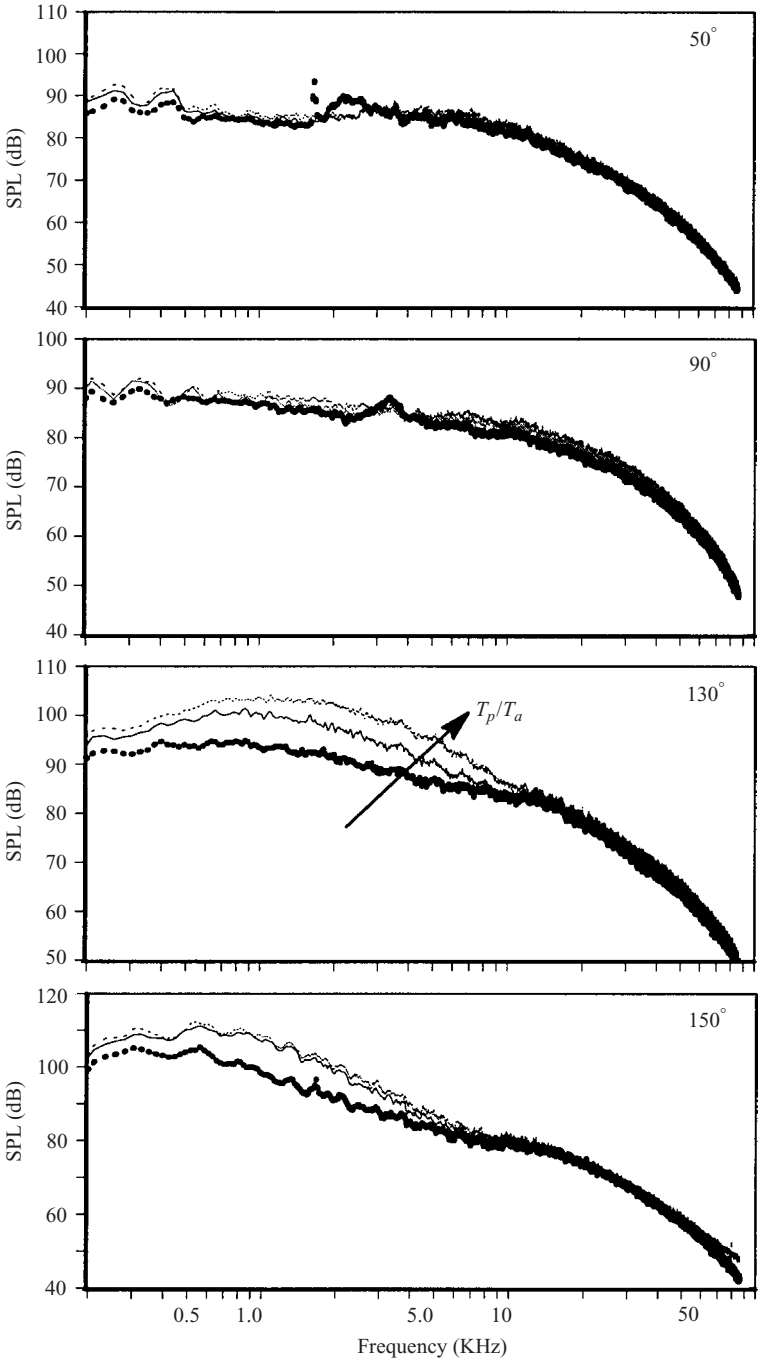

FIGURE 8. Effect of primary jet temperature with fixed secondary jet conditions. $NPR_s = 2.7$, $T_s/T_a = 1.0$, $NPR_p = 2.1$ Thick dotted line, $T_p/T_a = 1.0$ ($V_s/V_p = 1.14$); solid line, $T_p/T_a = 2.38$ ($V_s/V_p = 0.73$); thin dashed line, $T_p/T_a = 3.24$ ($V_s/V_p = 0.63$).

of the primary stream was slightly supersonic, in the range of 1.04 to 1.1. Tam & Tanna (1985*a*, *b*) provided a rationale for the observed minimum as follows. When the primary stream is subsonic and the secondary stream is supersonic, a shock-cell system

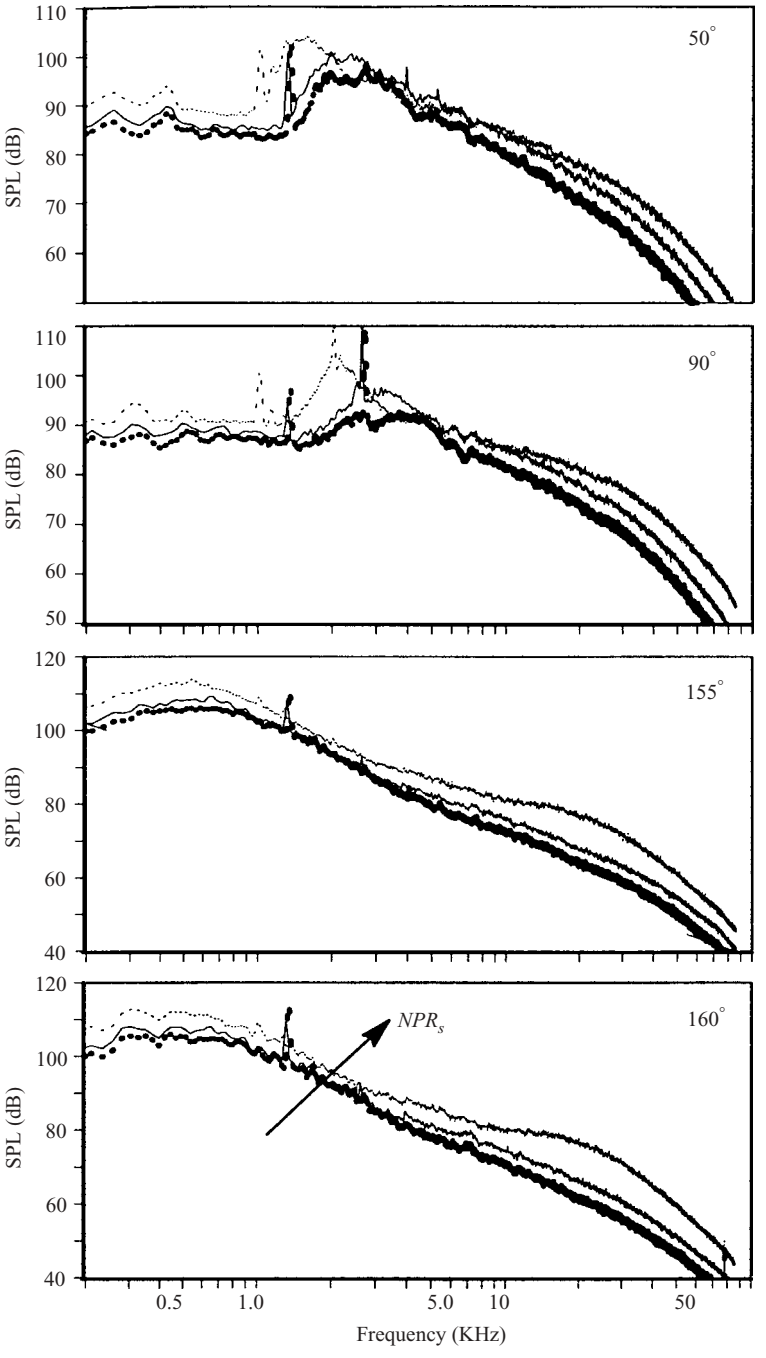

FIGURE 9. Spectral variation due to change in secondary stream with fixed primary jet conditions. $NPR_p = 3.0$, $T_p/T_a = 1.0$, $T_s/T_a = 1.0$. Thick dotted line, $NPR_s = 1.8$; solid line, $NPR_s = 2.1$; thin dashed line, $NPR_s = 3.0$.

can be maintained in the secondary stream. Since a subsonic flow cannot support shocks or discontinuities, the compression waves impinging on the inner shear layer are reflected back into the secondary stream as expansion waves. Depending on the

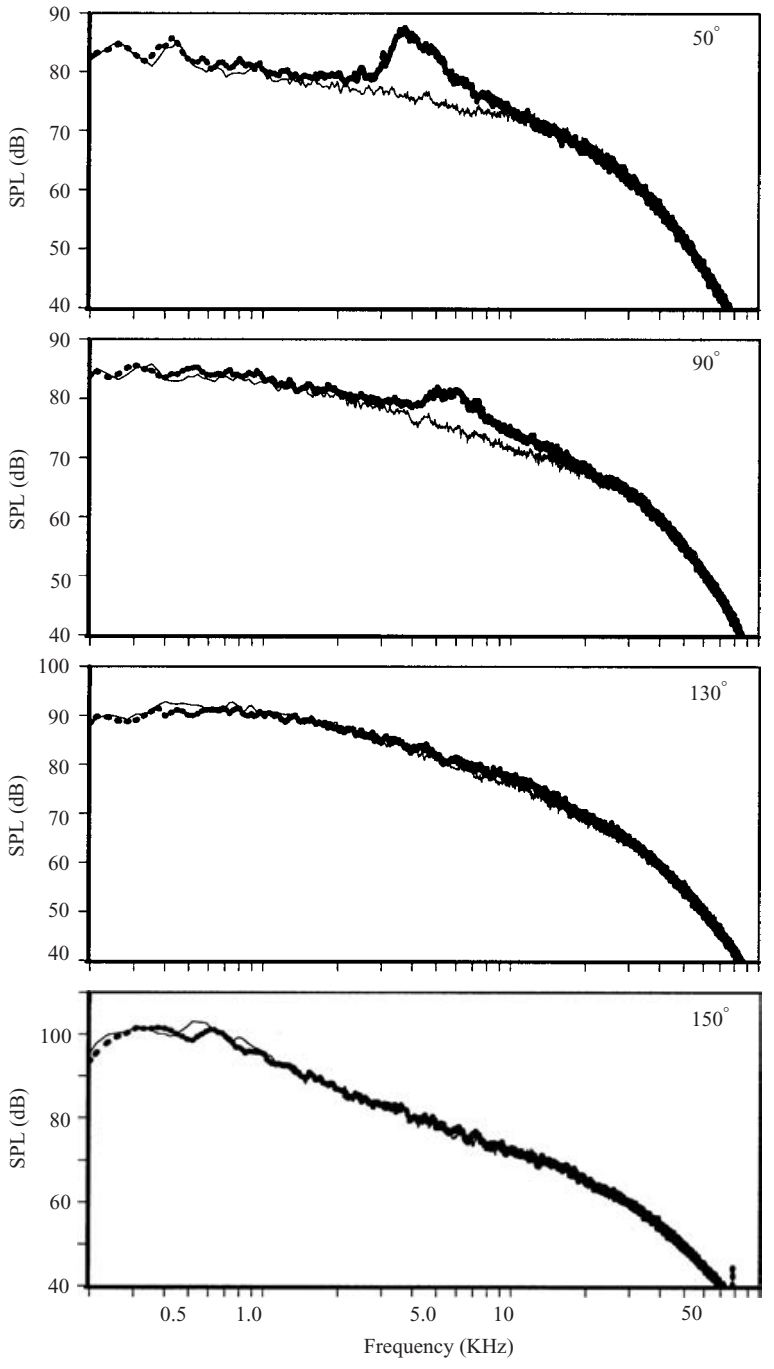

FIGURE 10. Spectral variation due to change in primary stream with fixed secondary conditions. $V_s/V_p = 1.0$, $NPR_s = 2.1$, $T_s/T_a = 1.0$. Solid line, $NPR_p = 1.4$, $T_p/T_a = 2.14$; thick dotted line, $NPR_p = 2.1$, $T_p/T_a = 1.0$.

shock strength, several shock cells may form, till the shock waves are dissipated in the downstream direction. However, when the primary stream is supersonic, part of the impinging wave is transmitted with a weaker reflection into the secondary stream.

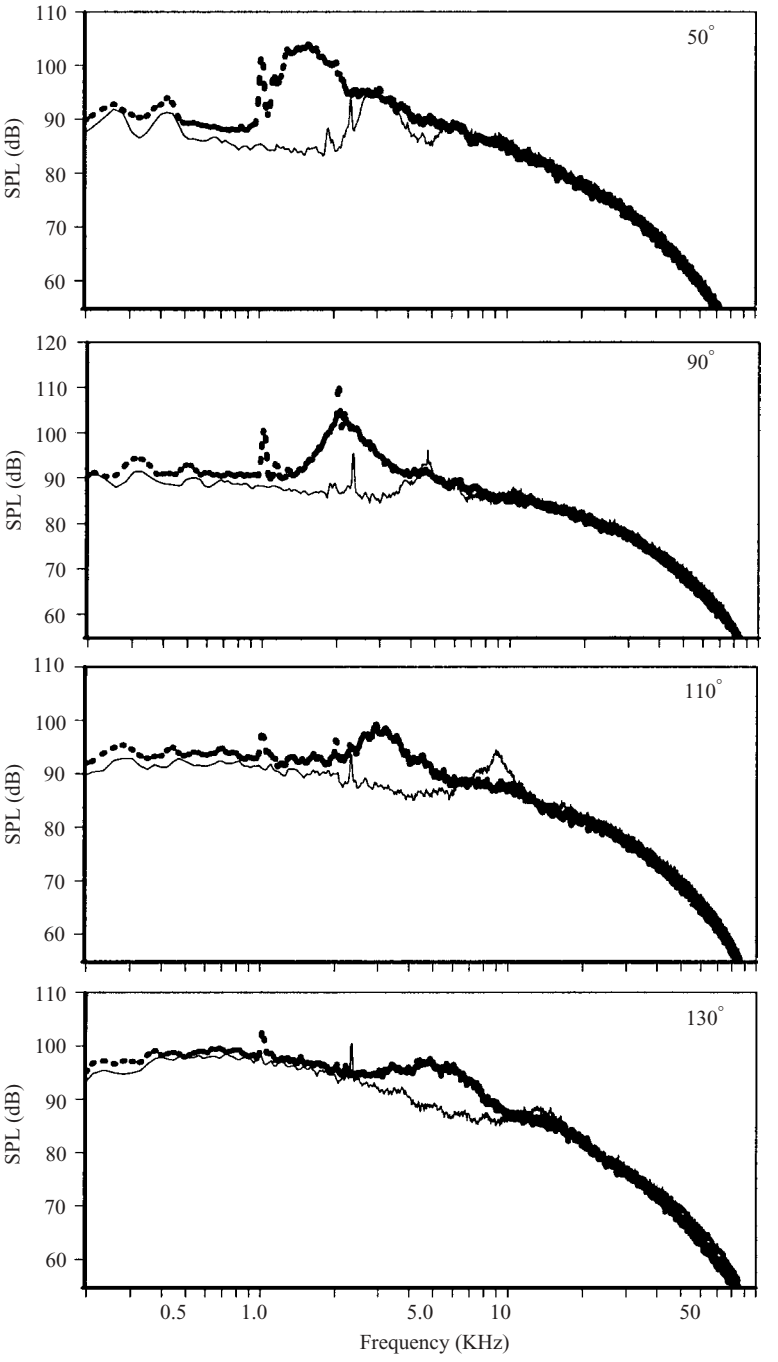

FIGURE 11. Spectral variation due to change in primary stream with fixed secondary conditions. $V_s/V_p = 1.0$, $NPR_s = 3.0$, $T_s/T_a = 1.0$. Solid line, $NPR_p = 1.6$, $T_p/T_a = 2.26$; thick dotted line, $NPR_p = 3.0$, $T_p/T_a = 1.0$.

After one or two reflections, the strength of the shock becomes negligible and the rate of decay of the shock amplitude in the axial direction is sufficient to preclude the formation of a multiple shock-cell system in the secondary stream. When there

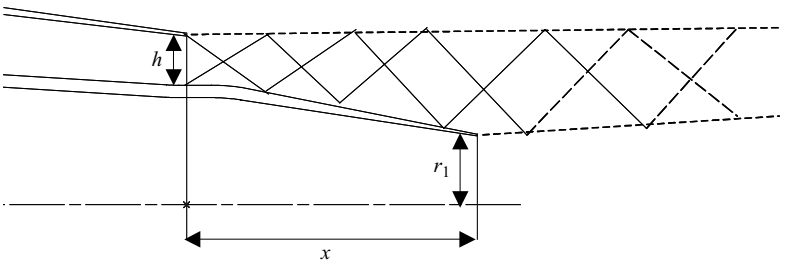

FIGURE 12. Sketch of the nozzle arrangement and possible shock-cell system in the secondary stream. $x/h = 6.09$, $h/r_1 = 0.718$.

are strong shocks in the primary stream, the influence of this shock-cell system would extend into the secondary stream and would lead to the generation of broadband shock-associated noise.

The Mach number of the primary stream in figures 5–8 is in the range of 1.04 to 1.09, a range at which no shock noise was observed in the data of Tanna *et al.* (1985). What then causes the shock–associated noise in the current results? An examination of the geometric details of the nozzle provides the likely explanation for the formation of shocks in the secondary stream at all Mach numbers for the primary jet. No schlieren pictures were acquired in the current test; however, one could infer from the acoustic data presented so far that shock cells with significant strength would have to be present in the secondary stream to account for the increase in noise when the secondary stream becomes supersonic. The nozzle used in Tanna *et al.* (1985) had an area ratio A_s/A_p of 0.747 and a recess ratio (defined as the ratio of the extension of the primary nozzle past the secondary nozzle to the annulus height) of 2.23. The geometric details of the current nozzle configuration are shown in figure 12. The area ratio of the current configuration is 3.0 and the recess ratio is 6.09. Furthermore, the ratio of the annulus height to the radius of the primary jet is 0.718. Thus, the thickness of the fan stream compared with the radius of the primary jet is not negligible for the current nozzle. The shock-cell structure is dependent on the geometric details and hence only a detailed analysis of the current configuration would provide the complete information. Though an extension of the analysis of Tam & Tanna (1985*a*, *b*) for the current geometry would provide more insights, the usefulness of a simple model for application to the cabin noise problem is not clear. First, detailed spectral characteristics at the aft angles are required. The levels of the shock peak in the aft directions are well below the peak of the jet mixing noise (by roughly 20 to 30 dB). Thus, the contributions of the shock-associated noise to total intensity would be negligible. Therefore, the development of equations for total intensity and peak frequency would not be adequate for practical applications. A computational approach or a more complex theory capable of predicting the spectra is necessary. Such a study is currently underway and will be reported elsewhere. Useful physical insights can still be gleaned with the following reasoning, while a comprehensive model, however desirable, is clearly beyond the scope of the current experimental program. However, if we confine ourselves within the framework of Tam & Tanna's analysis and assume that the length of the shock cell is of the order of the annulus height (see figure 3 in Tam & Tanna 1985*a*), it is conceivable that the present nozzle has three or more shock diamonds in the external plume. Given the large recess ratio, the supersonic secondary stream would expand to a local pressure that would be close to ambient pressure, and would not come into contact with the primary stream for several annulus heights downstream. When the secondary stream

does sense the supersonic primary stream, it could still take two or three reflections from the primary shear layer before the secondary shock-cell system decays. A cartoon of the possible scenario is also shown in figure 12. Thus, shocks could be established in the secondary stream regardless of the Mach number in the primary stream.

Apart from the details of the nozzle arrangement, the area ratio (A_s/A_p) is an important parameter in the noise generation process in a dual-stream jet. Sample results of the effect of area ratio on jet mixing noise, both under IVP and NVP conditions, were provided in Viswanathan (2002). It was pointed out in the preceding paragraph that the ratio of the annulus height to the radius of the primary jet for the current recessed geometry is 0.718. This ratio, which is related to the area ratio (A_s/A_p), could also be an important factor in the formation of shocks in the secondary stream. To illustrate this point, data are shown from a coplanar nozzle with the same flow areas and area ratio as the recessed nozzle. For the coplanar nozzle with area ratio of 3.0, the ratio of the annulus height to the radius of the primary jet is unity. Spectral comparisons at three angles from the coplanar and recessed nozzles are shown in figure 13. The operating conditions in the primary stream for the two geometries are comparable: $NPR_p = 3.0$ and $T_p/T_a = 3.0$ for the recessed nozzle and $NPR_p = 3.0$ and $T_p/T_a = 2.78$ for the coplanar nozzle. The NPR in the secondary stream has the same value of 1.8 for the two geometries. While the coplanar nozzle was operated with the secondary stream at a slightly elevated temperature ratio of 1.83, the temperature ratio in the secondary stream for the recessed nozzle was unity. Thus, there are some slight differences in the mixed velocity. Examination of the spectra for these cases, denoted by thick dotted and solid lines in figure 13, indicates that there is good agreement over a wide range of frequencies for the two geometries. There appears to be a screech tone for the coplanar case; further, the difference in level at the lower frequencies at the aft angles may be attributed to the higher mixed jet velocity for the coplanar case. Otherwise, the spectral shapes are very similar at all angles. Now, the secondary NPR is increased to 3.0 for the coplanar nozzle, while holding the other cycle conditions constant. At 50°, the increase in noise associated with this change in the cycle condition is similar to that observed for the recessed nozzle in figure 9. At the aft angles, there is a ~4 dB increase in level for the mixing noise at the lower frequencies, to the left of the spectral peak. However, there is a tremendous increase of 15 to 20 dB at the higher frequencies. Again, the magnitude of this increase is comparable to that seen for the recessed nozzle at the higher frequencies in the aft angles. It is worth noting that the supersonic secondary stream brought about this change and there is a strong indication that shock-associated noise from the secondary stream is responsible for the aft-radiating component. Thus, the ratio of the annulus height to the radius of the primary jet is seen to be an important parameter in the formation and modulation of shocks in the secondary stream. The geometric differences between the current nozzle and that of Tanna *et al.* (1985) could account for the observed differences in the characteristics of the shock-associated noise.

It is important to recognize that there is strong radiation of shock-associated noise to the aft angles. Data have been presented that point to the shocks in the secondary stream being responsible and that the frequency range is much higher than that associated with shocks in the forward quadrant. This finding, which has not been identified before, has profound implications for cabin noise. In several aircraft, it has been observed that there is an increase in noise levels in the cabin interior as one moves to the aft of the cabin. Though shock-associated noise was suspected to be responsible, the precise cause and the physics of the generation mechanism were not understood well.

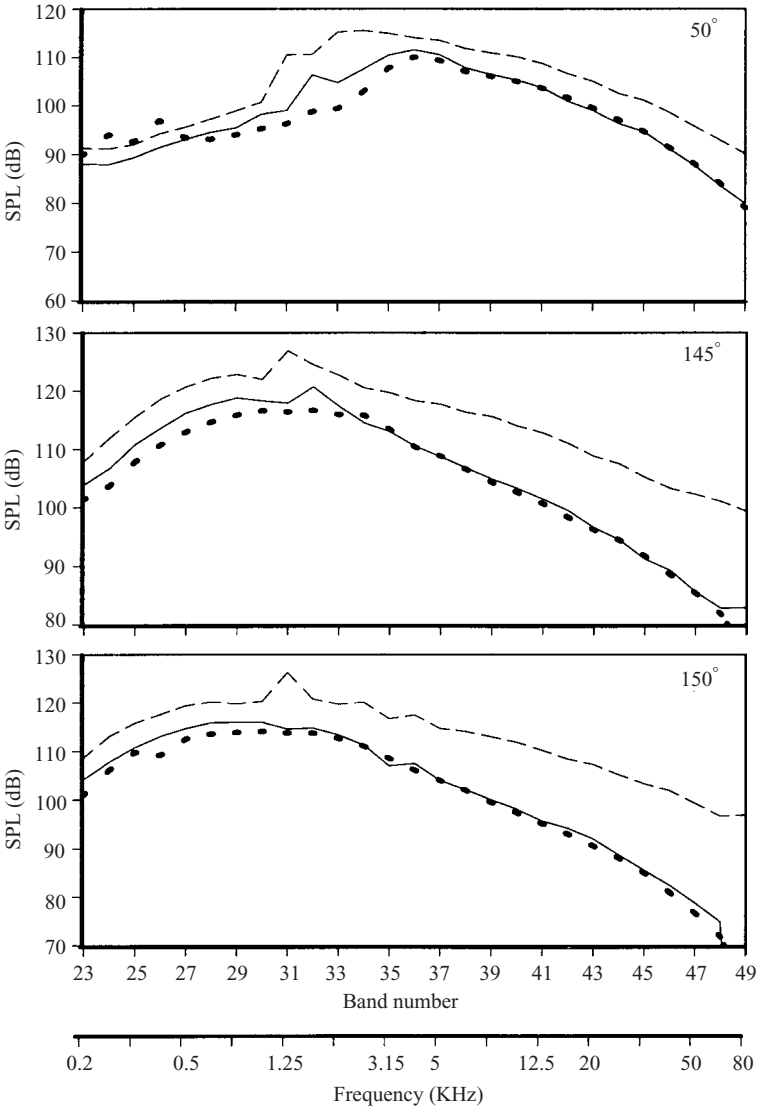

FIGURE 13. Comparison of spectra from recessed and coplanar nozzles. $A_s/A_p = 3.0$. Thick dotted line, recessed, $NPR_p = 3.0$, $T_p/T_a = 3.0$, $NPR_s = 1.8$, $T_s/T_a = 1.0$; solid line, coplanar, $NPR_p = 3.0$, $T_p/T_a = 2.78$, $NPR_s = 1.8$, $T_s/T_a = 1.83$; dashed line, coplanar, $NPR_p = 3.0$, $T_p/T_a = 2.78$, $NPR_s = 3.0$, $T_s/T_a = 1.83$.

In the results shown so far in this section, the velocity ratio V_s/V_p has been varied from 0.4 to 1.1, for the different combinations. However, the features of the shock-associated noise were not affected by the velocity ratio. This is especially striking in figure 8, where the effect of heating the primary jet was examined. The value of the velocity ratio dropped from 1.14 (IVP) to 0.63 (NVP) when the temperature ratio was increased from 1.0 to 3.24. Though the effect of the resulting increase in the mixed jet velocity can be observed on the mixing noise at aft angles, the change in shock-associated noise is minimal. Thus, unlike for mixing noise (see the Appendix), the effect of the velocity ratio on shock-associated noise is not significant.

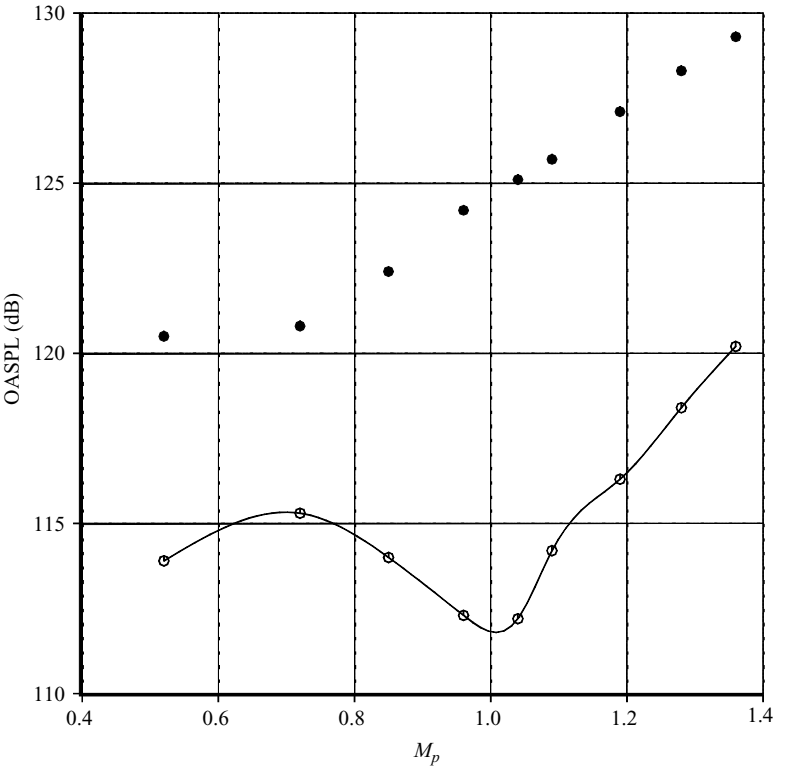

FIGURE 14. Variation of intensity with primary Mach number. $M_s = 1.36$. ○, 50°; ●, 150°.

In figure 14, the intensity of noise at two radiation angles of 50° and 150° is plotted as a function of primary Mach number while the secondary Mach number is held constant at 1.36 ($NPR_s = 3.0$). At 150°, where the mixing noise is dominant, there is a progressive increase in noise with primary Mach number, commensurate with an increase in the mixed jet velocity. However, at 50°, where shock-associated noise is dominant, the intensity attains a minimum when the primary Mach number is approximately unity. This result is similar to the one noted in Tam & Tanna (1985*a*). Examination of the spectra at 50° in figure 15 indicates that the spectral levels associated with the shock-associated noise are reduced when the primary Mach number is increased from 0.72 to 0.96. The intensity of the screech tone is also less. Furthermore, the peak frequency shifts to lower values when the primary Mach number is progressively increased from 0.7 to a value of 1.09 (only two cases are shown for the sake of clarity). At the lower Mach number, one can also identify three spectral peaks, attesting to the complex shock-cell structure responsible for the generation of the higher-order modes. With a further increase in Mach number, and attendant shocks in the primary jet, the situation becomes more complex and there is a broadening of the shock peak as seen in figure 9.

Finally in this section, we examine the variation of shock intensity (OASPL in fact, though the term intensity is loosely used here) with the Mach number of one of the streams fixed, while the other is varied. In figure 16, four sets of data are shown, with values of the secondary Mach number of 0.72, 0.96, 1.20 and 1.36. It has been established that the intensity of shock-associated noise from single-stream jets scales as $(M_p^2 - M_d^2)^2$. Also shown in figure 16 are lines that represent the theoretical

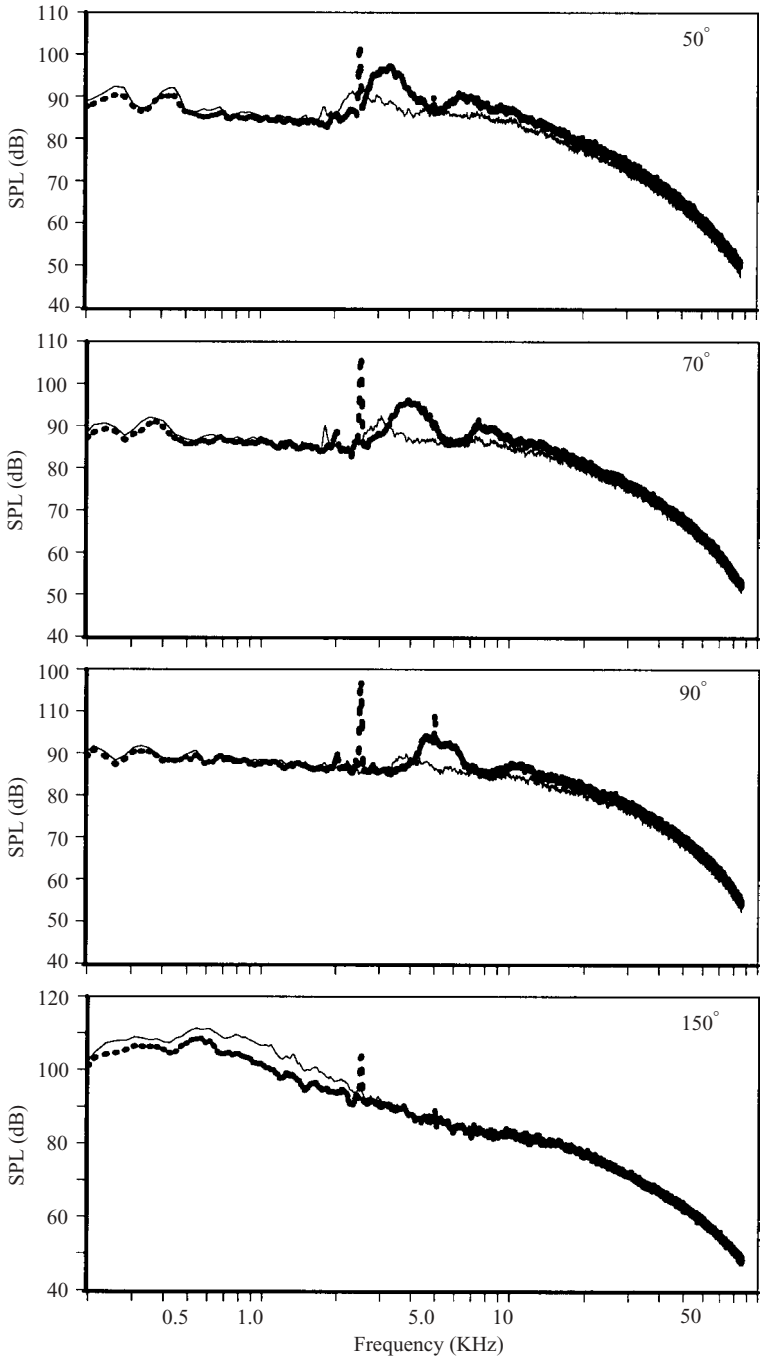

FIGURE 15. Effect of primary Mach number on shock-associated noise from the secondary stream. $NPR_s = 3.0$, $T_s/T_a = 1.0$. Thick dotted line, $NPR_p = 1.4$, $T_p/T_a = 2.14$; solid line, $NPR_p = 1.8$, $T_p/T_a = 2.37$.

variation of the intensity, calculated assuming a dependence of either $(M_p^2 - 1)^2$ or $(M_s^2 - 1)^2$. Note that convergent nozzles are used for both streams. When the Mach number of the secondary stream is supersonic, the measured intensities exhibit

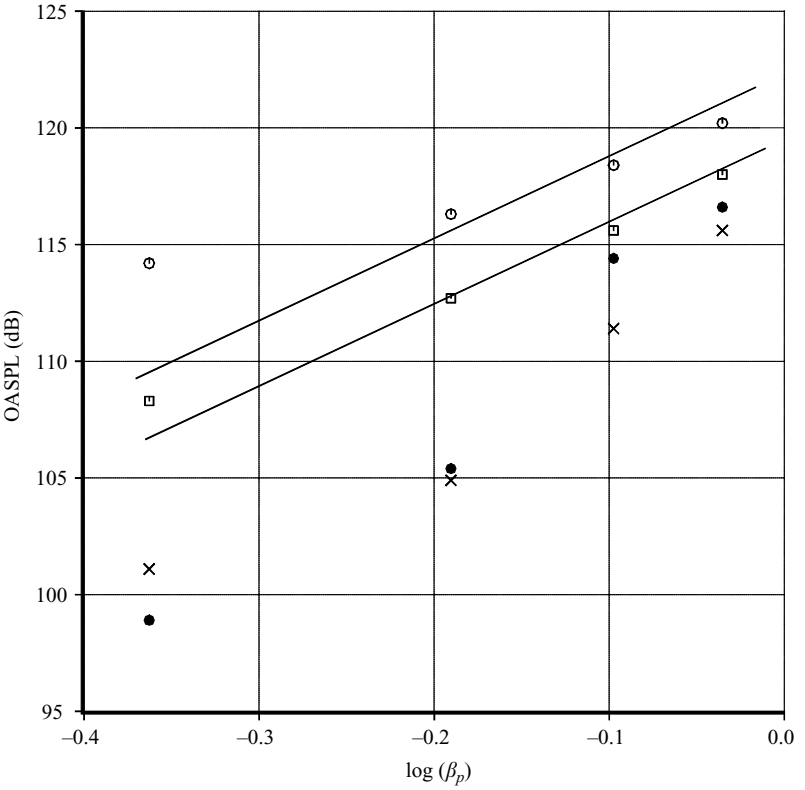

FIGURE 16. Variation of intensity at 50° with primary Mach number for fixed secondary Mach numbers. Lines: $(M_p^2-1)^2$. ●, $M_s=0.72$; ×, $M_s=0.96$; □, $M_s=1.20$; ○, $M_s=1.37$.

the theoretical variation. However, when the secondary stream is subsonic, no clear trend is apparent. Strong screech tones are observed at certain combinations of cycle conditions, as seen in figures 6 and 15, while they are absent when the NPR of one of the streams is altered slightly. Since these tones are part of the overall noise, no attempt has been made to remove them in the computation of overall levels. The presence of these tones could potentially cause the intensity of the shock-associated noise to be higher than the theoretical trend in the figures shown here.

In figure 17(*a*), four sets of data are again shown, with fixed primary Mach numbers of 0.72, 0.85, 0.96 and 1.09 while the secondary Mach number is varied. Note that the change in intensity is not very pronounced when the Mach number of the primary stream is varied in this range. Comparisons with the theoretical variation are shown in figure 17(*b*), where the curves have been spaced apart to enhance visual observation. Good agreement with the theoretical trend is seen at all primary Mach numbers. When the primary stream is highly supersonic (not shown here) there is no discernible trend.

4. Effect of forward flight

The effect of a co-flowing stream from the wind tunnel on the radiated noise is now investigated. It is customary to present these types of results such that the measured data at model scale are extrapolated to equivalent flyover conditions, with proper accounting for the effects of the propagation of sound through the tunnel shear layer.

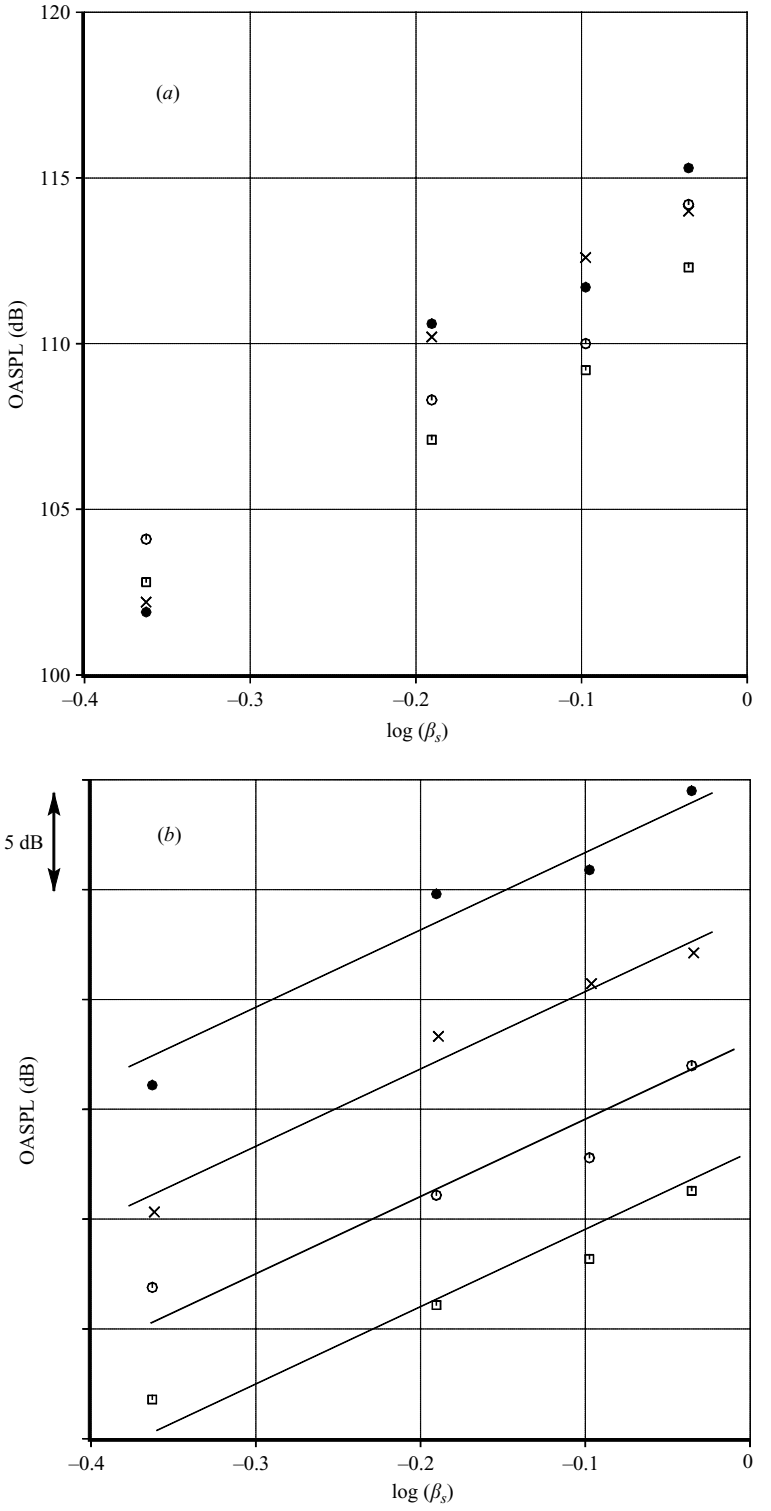

FIGURE 17. (*a*) Variation of intensity at 50° with secondary Mach number for fixed primary Mach numbers. ●, $M_p = 0.72$; ×, $M_p = 0.85$; □, $M_p = 0.96$; ○, $M_p = 1.09$. In (*b*) data for each M_p value have been separated for clarity and the lines show $(M_s^2 - 1)^2$.

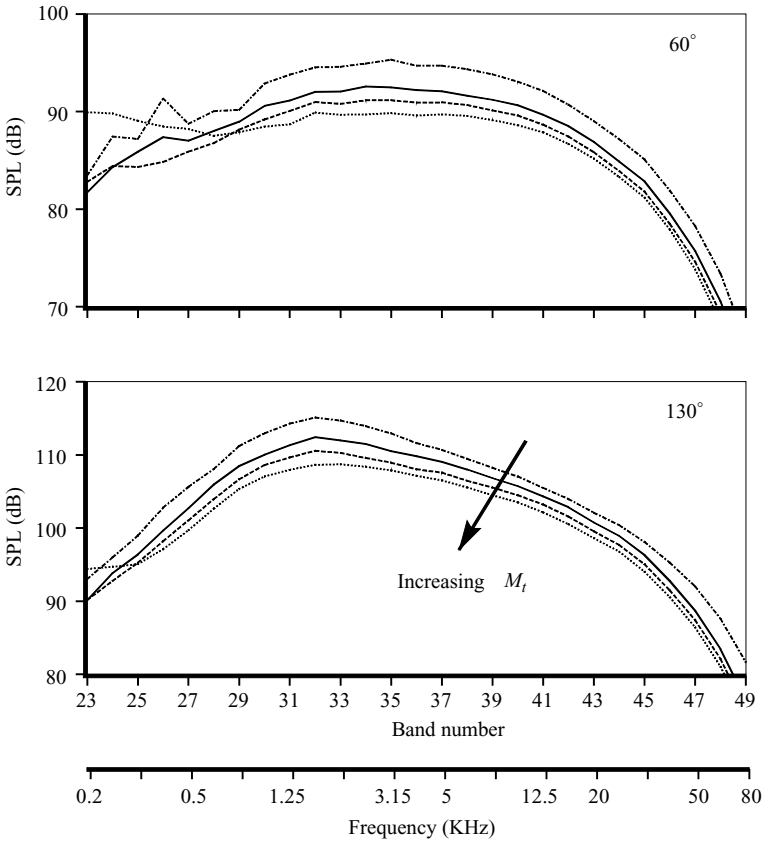

FIGURE 18. Effect of forward flight on mixing noise from single jet. $NPR_p = 1.89$, $T_p/T_a = 3.2$. Dot-dashed line, $M_t = 0$; solid line, $M_t = 0.16$; dashed line, $M_t = 0.24$; dotted line, $M_t = 0.32$.

Though validated methods are available to carry out this extrapolation, measured data are presented in a slightly different fashion here. Two effects are of paramount importance. One is due to the convection of an acoustic ray that emanates from the jet and subsequently has to propagate through the tunnel flow and the other is due to refraction by the tunnel shear layer, prior to reaching an observer in the far field. These two effects are opposite in sign: while the convection effect causes the acoustic ray to propagate to a larger angle in the downstream direction, the refraction effect bends the ray back in the upstream direction. For a given geometry of the jet and the wind tunnel, one can calculate these effects for any given tunnel Mach number. This is the procedure followed in the extrapolation process. Now, there are precisely two angles, one in the forward quadrant and one in the aft quadrant, where these two effects cancel each other. Direct comparison with the static data would be valid for these two angles, which have been estimated to be 60° and 130°. Additionally, the measured data at 145° for the wind-on case corresponds to the microphone at 150° for the static case. Hence, flight effects are shown at these three angles. However, it is not difficult to assess flight effects at any desired angle. Sample results on the effect of forward flight on turbulent mixing noise are included in the Appendix.

Before we examine the effect of forward flight on shock-associated noise from dual-stream nozzles, it is instructive to examine its effect on mixing and shock noise for a single-stream jet. In figure 18, spectra are shown at two angles for

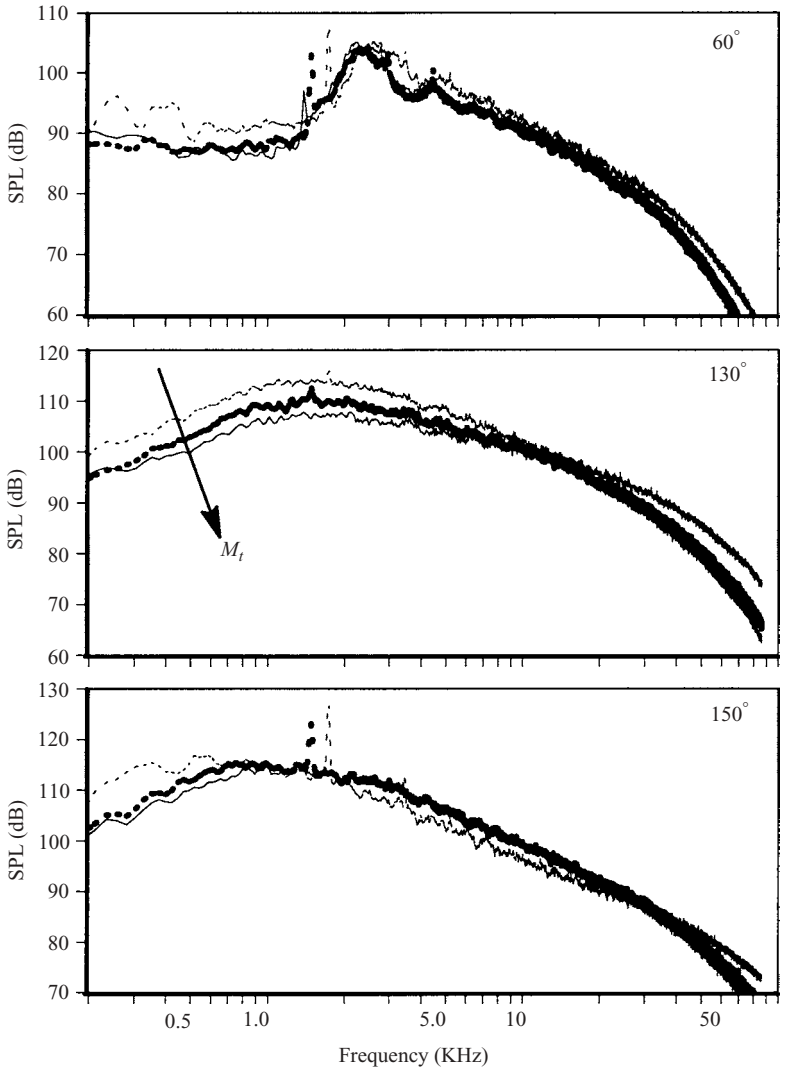

FIGURE 19. Effect of forward flight on shock-associated noise from single jet. $NPR_p = 3.5$, $T_p/T_a = 2.7$. Thin dashed line, $M_t = 0$; thick dotted line, $M_t = 0.24$; solid line, $M_t = 0.32$.

a jet at a Mach number of unity and temperature ratio 3.2, for four free-stream Mach numbers of 0, 0.16, 0.24 and 0.32. As expected, there is progressive reduction in level with increasing tunnel Mach number. There is a substantial reduction of $\sim$7 dB relative to the static case near the peak, when the tunnel Mach number is 0.32. In figure 19, similar comparisons are shown for a jet with a Mach number of 1.48 and temperature ratio of 2.7. There are some striking differences due to forward flight in the shock-associated noise. The reduction in level is $\sim$2 dB for the shock-associated noise at 60° in the mid-frequency range. In the aft directions, there is an increase in noise level in the mid-frequency range, while there is the usual reduction in mixing noise levels at the lower frequencies, seen clearly at 130°. Thus, the effect of forward flight on shock-associated noise is different from that on mixing noise.

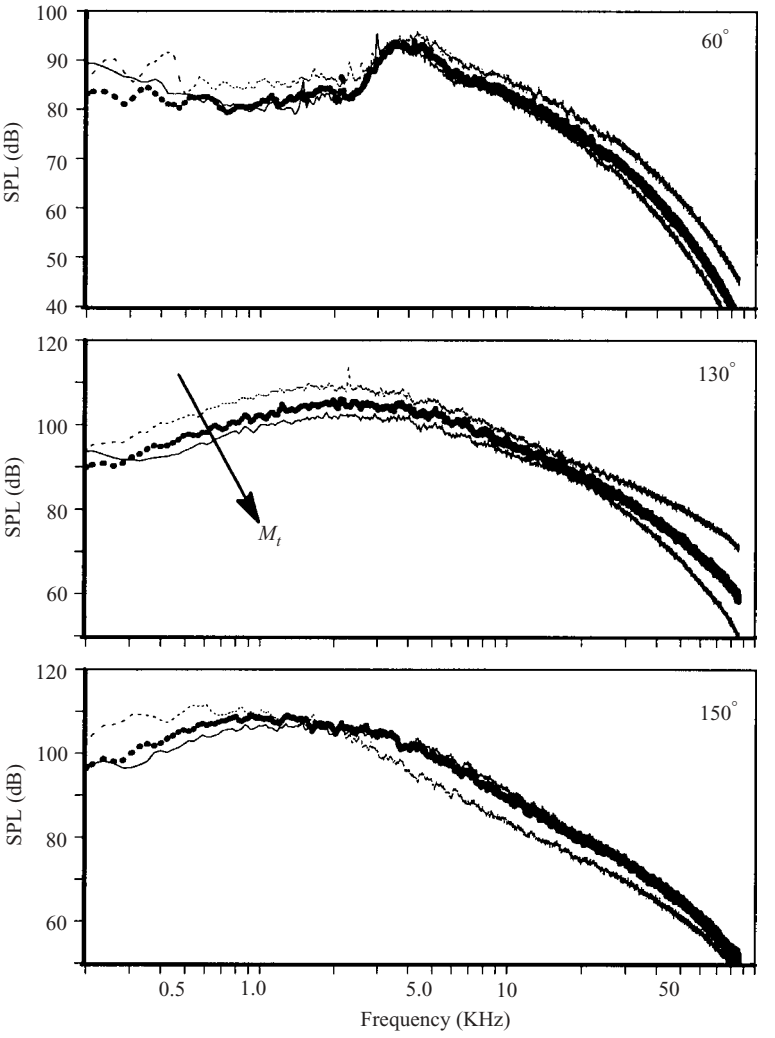

FIGURE 20. Effect of forward flight on shock-associated noise. $NPR_p = 3.0$, $T_p/T_a = 3.04$, $NPR_s = 1.6$. Thin dashed line, $M_t = 0$; thick dotted line, $M_t = 0.24$; solid line, $M_t = 0.32$.

Figure 20 shows the flight effect when the secondary stream is operated at a subsonic Mach number of 0.85, with $NPR_p = 3.0$ ($M_p = 1.37$) and $T_p/T_a = 3.04$. The observed trends are very similar to those for a single jet seen in figure 19. When the secondary stream is supersonic with $M_s = 1.37$ and primary stream subsonic ($M_p = 0.85$, $T_p/T_a = 2.37$), there is a dramatic difference, as shown in figure 21. First, there is no change in level for the broadband shock-associated noise at 60°, while the screech tone is amplified. At 130°, there is strong amplification of the shock peak with increasing tunnel Mach number, while there is no change in level to the right of the peak. Similar trends are seen at 150°, though the level of the mixing noise for the static case somewhat masks the amplification of the shock peak. When the Mach number of the primary stream is increased to 1.37 in figure 22, with shocks in the primary stream as well, the flight effects exhibit traits that are a combination of those

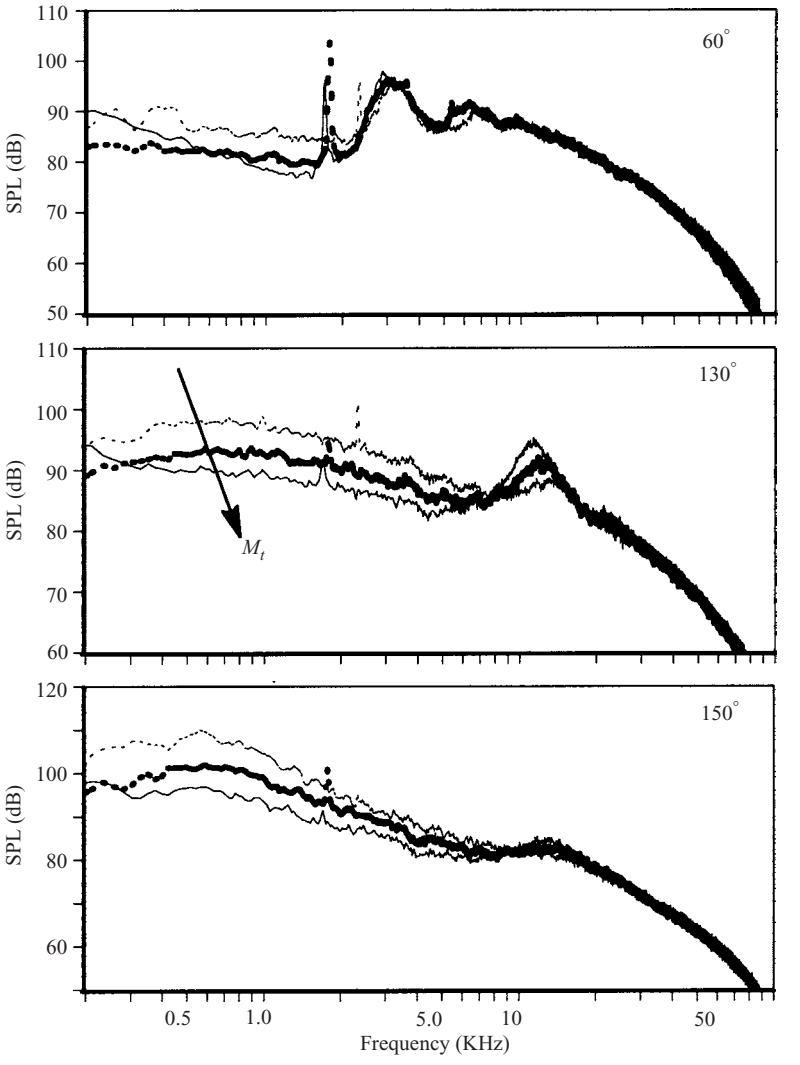

FIGURE 21. Effect of forward flight on shock-associated noise. $NPR_p = 1.6$, $T_p/T_a = 2.26$, $NPR_s = 3.0$. Thin dashed line, $M_t = 0$; thick dotted line, $M_t = 0.24$; solid line, $M_t = 0.32$.

seen in figures 20 and 21. There is a slight reduction at 60° at the higher frequencies, while there is a slight amplification of the shock peaks at the aft angles. The primary stream is unheated in figure 22. Similar effects are observed when the temperature of the primary stream is increased (not shown here), though the increase in mixing noise due to heating masks the shock noise. In all these figures, the frequency of the screech tone decreases with increasing free-stream Mach number. Furthermore, the peak frequency of broadband shock-associated noise has a lower value, the spectral peak becomes narrower and several higher-order peaks become prominent with increasing flight speed. Similar effects for single jets are observed in figure 19 and have been reported by Drevet, Duponchel & Jacques (1977), Norum & Shearin (1988) and Norum & Brown (1993), among others.

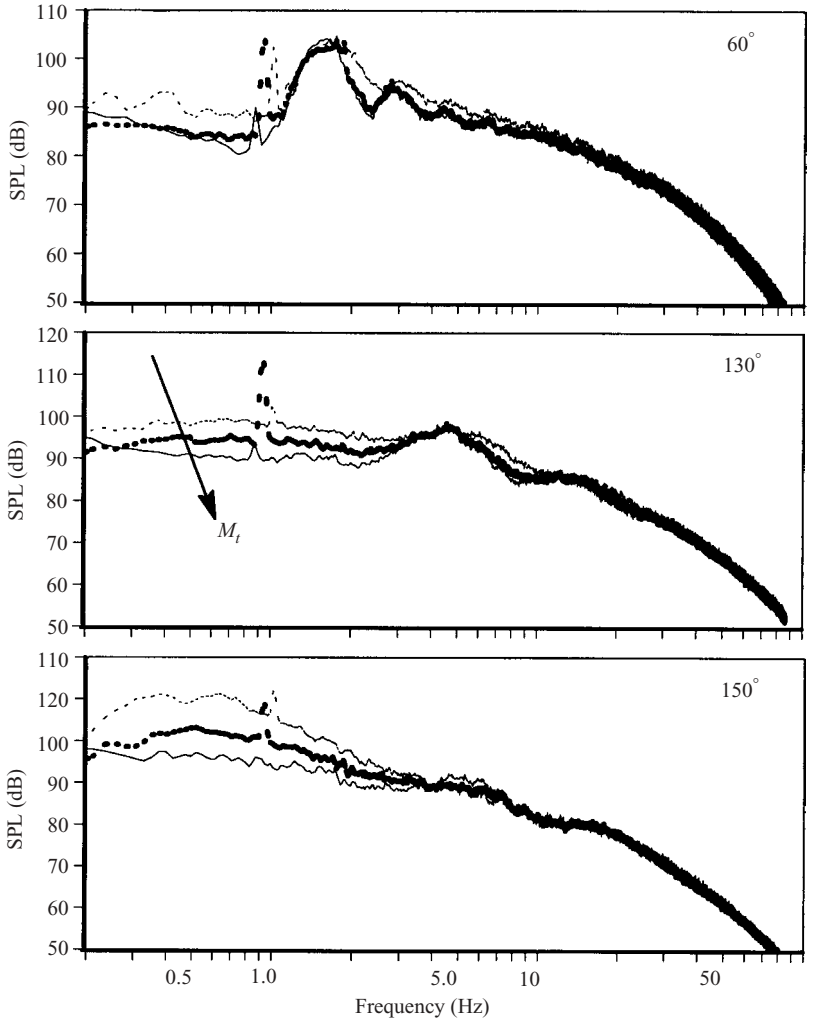

FIGURE 22. Effect of forward flight on shock-associated noise. $NPR_p = 3.0$, $T_p/T_a = 1.0$, $NPR_s = 3.0$. Thin dashed line, $M_t = 0$; thick dotted line, $M_t = 0.24$; solid line, $M_t = 0.32$.

5. Summary

An extensive study of noise from dual-stream nozzles has been carried out to assess the characteristics of the different sources in terms of their frequency content and their principal radiation directions. The spectral variations, due to changes in the operating conditions of the two streams, in turbulent mixing noise and shock-associated noise have been quantified experimentally under static conditions as well as in the presence of a co-flowing stream. The geometry of the nozzle chosen for this study has an area ratio of 3.0, with the secondary nozzle recessed in relation to the exit of the primary nozzle, and is representative of the arrangement of the nozzles in current high-bypass ratio engines. The salient conclusions, both for turbulent mixing noise (from the Appendix) and shock-associated noise are listed below.

The present results confirm the influence of the velocity ratio on mixing noise. At low velocity ratios, there is an increase in level across the entire spectrum in the forward quadrant and near-normal angles when either the primary or secondary

velocity is increased. The magnitude of the increase at the lower angles is also nearly uniform across the spectrum. At higher velocity ratios, when the strength of the outer shear layer is much stronger, there is no change in spectral level at the higher frequencies at all angles, indicating that the secondary shear layer is responsible for this portion of the generated noise. However, in the aft directions, there is a substantial increase in noise at the low and mid frequencies, with the increase more pronounced at lower velocity ratios. It is believed that the fully merged jet is responsible for the generation of the low- and mid-frequency noise. When the velocity of the primary stream is increased, the velocity of the mixed jet increases, directly leading to an increase in the low-frequency noise. At low velocity ratios, when the velocity in the secondary stream is increased with a fixed velocity in the primary stream, there is a reduction in the mid-frequency levels at the aft angles.

It is recognized that the area ratio is an important parameter and the above trends could be somewhat different at lower values of area ratio. Needless to say, there are several competing (or coexistent) mechanisms that produce the observed trends. The effects of source location, source strength, source convection, shielding and refraction are all important in the noise generation and radiation process. In a dual-stream nozzle, the individual effects are harder to assess and quantify.

Currently, there is limited understanding of the mechanisms responsible for the generation of shock-associated noise from dual-stream nozzles. This state of knowledge is not unexpected, given the paucity of experimental data from realistic geometries that would lead to a better understanding of the problem. There are tremendous differences in the radiated noise depending upon the establishment of shocks in the primary, or secondary or both streams. When the primary stream is supersonic, with the secondary stream at subsonic or low supersonic Mach number, the shock-associated noise from the primary jet controls the radiated noise to all angles. The characteristics of the shock-associated noise are similar to those from a single jet and the importance of the secondary shear layer is presumably diminished greatly. Dramatic differences occur when the secondary stream is supersonic and the primary stream is either subsonic or at a low supersonic Mach number. The emergence of shock-associated noise from the secondary stream becomes apparent in the forward angles. However, of greater significance is the radiation of shock-associated noise to large aft angles, which becomes more pronounced with increasing Mach number in the secondary stream. This trend has not been reported in the past. Conclusive evidence is presented that indicates that strong radiation to aft angles happens only when the secondary stream is supersonic, regardless of the Mach number of the primary stream. In this regard, the characteristics of the shock-associated noise from the secondary stream are very different from those of a single jet or a dual-stream jet with the shocks in the primary jet.

The effect of the jet temperature of the primary stream on radiated noise is also different depending on the Mach number of the secondary stream. When the secondary stream is subsonic with the primary stream slightly supersonic, there is a near-uniform increase in level across the spectra at lower angles, with a substantial increase in the levels of the mixing noise at aft angles commensurate with the higher mixed velocity. The situation is very different when the secondary stream is supersonic. There is a small increase in the levels at the lower frequencies at the lower angles, while there are no changes in levels at the higher frequencies at all angles even when the temperature of the primary stream is increased by a factor of 3.24. Therefore, the shock-associated noise from the secondary stream is the dominant source when the primary stream is subsonic or at a low supersonic Mach number. When strong shocks

are present in both the streams there is a broadening of the shock peak at lower angles and a change in the peak frequency, caused perhaps by the complex interaction of the shock-cell structure in the two streams. Unlike for mixing noise, the effect of velocity ratio is negligible once strong shocks are present in either stream.

The geometric details of the nozzle arrangement are important in the formation of shocks in the secondary stream, though the Mach number of the primary stream could play a role in the dissipation of the shocks once the two streams come into contact. Even in the range of Mach numbers (1.04 to 1.1) for which no shock-associated noise was observed in a previous study, a significant contribution is noted in the current investigation. A reason for the current trends, based on the importance of the geometric parameters of recess ratio and the ratio of the annulus height to that of the radius of the primary jet, has been proposed. The intensity of the shock-associated noise at the lower angles, in general, is proportional to the strength of the shocks and scales with either $(M_p^2 - 1)^2$ or $(M_s^2 - 1)^2$. There is good correlation, especially with the secondary Mach number, when the primary stream is either subsonic or slightly supersonic.

Just as for a single jet, the effect of forward flight on mixing noise and shock-associated noise is very different. The usual reduction in level, the magnitude of which increases with increasing flight velocity, is observed for the mixing noise. The effects for a dual-stream jet with the primary jet being supersonic are similar to those of a single supersonic jet. There is substantial amplification of the shock peak, especially at the aft angles, when the secondary stream is supersonic. In general, the frequency of the screech tone decreases with increasing free-stream Mach number regardless of the presence of the shock in either the primary or secondary stream. Furthermore, the spectral peak becomes narrower and several higher-order peaks become prominent with increasing flight speed.

The radiation of shock-associated noise to the aft angles is of great concern because of the transmission of this component into the rear of the cabin. As seen here, the effect due to forward flight further exacerbates this problem. Even though the Mach numbers of the flight stream in this study are much lower than that at cruise, the amplification of the second hump could be more severe at cruise conditions if the current trends hold true. A better understanding and means to reduce this component are clearly needed, as this is a practical problem for certain aircraft.

It is a pleasure to thank Dr M. C. Joshi for several insightful comments and editorial suggestions, which improved this article. The diligence and the enthusiastic support of the LSAF test crew are appreciated greatly.

REFERENCES

Balsa, T. F. & Gliebe, P. R. 1977 Aerodynamics and noise of coaxial jets. *AIAA J.* **15**, 1550–1558.

Bridges, J. 2002 Measurements of turbulent flow field in separate flow nozzles with enhanced mixing devices. *NASA TM*-2002-211366.

Bridges, J. & Wernet, M. P. 2003 Measurements of the aeroacoustic sound source in hot jets. *AIAA Paper* 2003-3130.

Cocking, B. J. 1976 An experimental study of coaxial jet noise. *NGTE Rep.* 333.

Crouch, R. W., Coughlin, C. L. & Paynter, G. C. 1976 Nozzle exit flow profile shaping for jet noise reduction. *AIAA Paper* 76-511.

Dosanjh, D. S., Bhutiani, P. K. & Ahuja, K. K. 1978 Supersonic jet noise suppression by coaxial cold/heated jet flows. *AIAA J.* **16**, 268–270.

Dosanjh, D. S., Yu, J. C. & Abdelhamid, A. N. 1971 Reduction of noise from supersonic jet flows. *AIAA J.* **9**, 2346–2353.

Drevet, P., Duponchel, J. P. & Jacques, J. R. 1977 The effect of flight on jet noise as observed on the Bertin Aérotrain. *J. Sound Vib.* **54**, 173–201.

Fisher, M. J., Preston, G. A. & Mead, C. J. 1998*a* A modelling of the noise from simple coaxial jets, Part I: With unheated primary flow. *J. Sound Vib.* **209**, 385–403.

Fisher, M. J., Preston, G. A. & Mead, C. J. 1998*b* A modelling of the noise from simple coaxial jets, Part II: With heated primary flow. *J. Sound Vib.* **209**, 405–417.

Goodykoontz, J. H. & Stone, J. R. 1979 Experimental study of coaxial nozzle exhaust noise. *AIAA Paper* 79-0631.

Harper-Bourne, M. & Fisher, M. J. 1973 The noise from shock waves in supersonic jets. *AGARD-CP*-131, pp. 1–13.

Knott, P. R., Stringas, E. J., Brausch, J. F., Staid, P. S., Heck, P. H. & Latham, D. 1978 Acoustic tests of duct-burning turbofan jet noise simulation. *NASA CR*-2966.

Kozlowski, H. & Packman, A. B. 1976 Aeroacoustic tests of duct-burning turbofan exhaust nozzles. *NASA CR*-2628.

Larson, R. S. 1979 A jet exhaust noise prediction procedure for inverted velocity profile coannular nozzles. *AIAA Paper* 79-0633.

Lu, H. Y. 1983 Effect of excitation on coaxial jet noise. *AIAA J.* **21**, 214–220.

Lu, H. Y. 1986 An empirical model for prediction of coaxial jet noise in ambient flow, *AIAA Paper* 86-1912.

Olsen, W. A. & Friedman, R. 1974 Jet noise from coaxial nozzles over a wide range of geometric and flow parameters. *AIAA Paper* 74-43.

Norum, T. D. & Brown, M. C. 1993 Simulated high speed flight effects on supersonic jet noise. *AIAA Paper* 93-4388.

Norum, T. D. & Seiner, J. M. 1982*a* Measurements of static pressure and far field acoustics of shock-containing supersonic jets. *NASA TM* 84521.

Norum, T. D. & Seiner, J. M. 1982*b* Broadband shock noise from supersonic jets. *AIAA J.* **20**, 68–73.

Norum, T. D. & Shearin, G. 1988 Shock structure and noise of supersonic jets in simulated flight to Mach 0.4. *NASA TP*-2785.

Pao, S. P. 1979 A correlation of mixing noise from coannular jets with inverted flow profiles. *NASA TP*-1301.

Reed, D. H., Bhat, T. R. S. & Conley, W. T. 1999 Industry perspective on jet noise – prediction and reduction requirements. *J. Acoust. Soc. Am.* **105**, 951.

SAE 1994 Gas turbine jet exhaust noise prediction. Society of Automotive Engrs ARP876, Revision D.

Salikuddin, M. 1995 Shock-associated and turbulent mixing jet noise for coannular nozzle. *CEAS/AIAA Paper* 95-016.

Seiner, J. M. 1984 Advances in high speed jet aeroacoustics. *AIAA Paper* 84-2275.

Seiner, J. M. 2003 Advances in jet noise measurement techniques. *AIAA Paper* 2003-0711.

Seiner, J. M. & Norum, T. D. 1979 Experiments on shock associated noise of supersonic jets. *AIAA Paper* 79-1526.

Seiner, J. M. & Norum, T. D. 1980 Aerodynamic aspects of shock containing jet plumes. *AIAA Paper* 80-0965.

Shields, F. D. & Bass, H. E. 1977 Atmospheric absorption of high frequency noise and application to fractional-octave band. *NASA CR* 2760.

Stone, J. R. 1977 An empirical model for inverted-velocity-profile jet noise prediction. *NASA TM*-73838.

Stone, J. R., Groesbeck, D. E. & Zola, C. L. 1983 Conventional profile coaxial jet noise prediction. *AIAA J.* **21**, 336–342.

Stone, J. R., Zola, C. L. & Clark, B. J. 1999 An improved model for conventional and inverted-velocity-profile coannular jet noise. *AIAA Paper* 99-0078.

Tam, C. K. W. 1987 Stochastic model theory of broadband shock associated noise from supersonic jets. *J. Sound Vib.* **116**, 265–302.

Tam, C. K. W. 1991 Jet noise generated by large-scale coherent motion. In *Aeroacoustics of Flight Vehicles: Theory and Practice, Volume 1: Noise Sources* (ed. H. H. Hubbard). NASA RP-1258, pp. 311–390.

Tam, C. K. W. & Tanna, H. K. 1982 Shock associated noise of supersonic jets from convergent-divergent nozzles. *J. Sound Vib.* **81**, 337–358.

Tam, C. K. W. & Tanna, H. K. 1985*a* Shock associated noise of inverted-profile coannular jets, Part II: Condition for minimum noise. *J. Sound Vib.* **98**, 115–125.

Tam, C. K. W. & Tanna, H. K. 1985*b* Shock associated noise of inverted-profile coannular jets, Part III: Shock structure and noise characteristics. *J. Sound Vib.* **98**, 127–145.

Tanna, H. K. 1980 Coannular jets – are they really quiet and why? *J. Sound Vib.* **72**, 97–118.

Tanna, H. K., Brown, W. H. & Tam, C. K. W. 1985 Shock associated noise of inverted-profile coannular jets, Part I: Experiments. *J. Sound Vib.* **98**, 95–113.

Tanna, H. K. & Morris, P. J. 1985 The noise from normal-velocity-profile coannular jets. *J. Sound Vib.* **98**, 213–234.

Tanna, H. K., Tester, B. J. & Lau, J. C. 1979 The noise and flow characteristics of inverted-profile coannular jets. *NASA CR*-158995.

Viswanathan, K. 2002 Analysis of the two similarity components of turbulent mixing noise. *AIAA J.* **40**, 1735–1744.

Viswanathan, K. 2003 Jet aeroacoustic testing: issues and implications. *AIAA J.* **41**, 1674–1689.

Viswanathan, K. 2004 Aeroacoustics of hot jets. *J. Fluid Mech.* **516**, 39–82.

Williams, T. J., Ali, M. R. H. & Anderson, J. S. 1969 Noise and flow characteristics of coaxial jets. *J. Mech. Engng Sci.* **11**, April, 133–142.

Yamamoto, K., Brausch, J. F., Janardan, B. A., Hoerst, D. J., Price, A. O. & Knott, P. R. 1984 Experimental investigation of shock-cell noise reduction for single-stream nozzles in simulated flight. *Test Nozzles and Acoustic Data, Comprehensive Data Report*, Vol. 1. *NACA CR*-168234.